~~CONFIDENTIAL~~

NASA TECHNICAL MEMORANDUM

CLASSIFICATION CHANGE

NASA TM X-53398

February 23, 1966

To ______________

By authority of CDS Gp 4

Changed by [illegible] Date 12/4/74

Classified Document Master Control Station, NASA
Scientific and Technical Information Facility

N79-76290

(NASA-TM-X-53398) SATURN I BLOCK II GUIDANCE SUMMARY REPORT (NASA) 48 p

Unclas

00/18 11013

NASA TM X-53398

FACILITY FORM: TMX-53398 (NASA CR OR TMX OR AD NUMBER)

(CODE)

21 (CATEGORY)

SATURN I BLOCK II GUIDANCE SUMMARY REPORT

By R. A. CHAPMAN
Aero-Astrodynamics Laboratory

~~NOTICE — THIS DOCUMENT CONTAINS INFORMATION AFFECTING THE NATIONAL DEFENSE OF THE UNITED STATES WITHIN THE MEANING OF THE ESPIONAGE LAWS, TITLE 18, U.S.C., SECTIONS 793 AND 794. ITS TRANSMISSION OR THE REVELATION OF ITS CONTENTS IN ANY MANNER TO AN UNAUTHORIZED PERSON IS PROHIBITED BY LAW.~~

NASA

George C. Marshall Space Flight Center, Huntsville, Alabama

~~GROUP 4
Downgraded at 3 year intervals; declassified after 12 years~~

[redacted]

SECURITY NOTE

This document contains information affecting the national defense of the United States within the meaning of the Espionage Law, Title 18, U.S.C., Section 793 and 794, as amended. The transmission or revelation of its contents in any manner to an unauthorized person is prohibited by law.

C66-2586

TECHNICAL MEMORANDUM X-53398

SATURN I BLOCK II GUIDANCE SUMMARY REPORT

By

R. A. Chapman

George C. Marshall Space Flight Center

Huntsville, Alabama

ABSTRACT

One of the missions assigned to the Saturn I Block II vehicles was flight testing the ST-124 inertial guidance system. This is an analytic report of the ST-124 platforms and associated hardware flown on the six Saturn I Block II vehicles, SA-5 through SA-10.

This report presents for each vehicle the velocity component errors versus time for the total powered flight, combinations of platform system errors that would produce the velocity error profiles, and the velocity component error corresponding to each platform system error.

NASA - GEORGE C. MARSHALL SPACE FLIGHT CENTER

[redacted]

NASA - GEORGE C. MARSHALL SPACE FLIGHT CENTER

TECHNICAL MEMORANDUM X-53398

February 23, 1966

SATURN I BLOCK II GUIDANCE SUMMARY REPORT

By

R. A. Chapman

AERO-ASTRODYNAMICS LABORATORY

RESEARCH AND DEVELOPMENT OPERATIONS

[redacted]

[redacted]) TABLE OF CONTENTS

(U) LIST OF ILLUSTRATIONS

(U) LIST OF TABLES

(U) DEFINITION OF SYMBOLS

Symbol	Definition
B	Acceleration bias
M_{pq}	Misalignment of the sensitive axis of the pth accelerometer about the qth axis.
δ_x	Initial platform leveling error in yaw
δ_y	Initial azimuth error
δ_z	Initial platform leveling error in pitch
$\dot{\delta}_{x,y,z,}$	Constant drift rate of X,Y,Z gyros respectively.
$\dot{\delta}_{x/\ddot{x}},\ \ _{y/\ddot{y}}$	"g"-sensitive drift due to mass unbalance along the spin reference axis (X and Y gyros respectively).
$\dot{\delta}_{x/\ddot{y}},\ \ _{y/\ddot{x}},\ \ _{z/\ddot{y}}$	Drift due to end plate "g"-sensitive turbine torque (X,Y,Z gyros respectively).
$\dot{\delta}_{z/\ddot{x}}$	"g"-sensitive drift due to mass unbalance along input axis of Z gyro
$S_{x,y}$	Scale factor error of range and altitude accelerometers respectively.
i	Refers to ith row
j	Refers to jth column

[redacted]

TECHNICAL MEMORANDUM X-53398

SATURN I BLOCK II GUIDANCE SUMMARY REPORT

[redacted]) SUMMARY

This report presents an error analysis of the ST-124 inertial platform systems flown on the Saturn I Block II flights. Final data from precision tracking were used for comparisons with the telemetered guidance velocities. These differences were input to a weighted Least Squares Program to determine the most probable sets of platform system errors. The error solutions were verified by adjusting the telemetered velocities and computing a continuous trajectory comparable to the reference trajectory and satisfying the orbital insertion conditions.

Although some platform system errors were larger than desired for a precision flight, averages for the six Saturn I Block II flights indicated only the "g"-sensitive gyro drifts were greater than the 3σ value specifications. The average error was 0.07 deg/hr/g compared to a 3σ value of 0.05 deg/hr/g. However, sixteen of twenty-four "g"-sensitive drift terms were predicted greater than the error analysis indicated.

The flight tests indicated each guidance system performed to a high degree of accuracy.

[redacted]

[redacted]

[redacted] 1.0 INTRODUCTION

One of the missions assigned to the Saturn I Block II vehicles was flight testing the ST-124 inertial guidance system. This is an analytic report of the ST-124 stable platforms and associated hardware flown on six Saturn I Block II vehicles, Saturn SA-5 through SA-10.

The analyses presented in this report are based on comparisons of the telemetered guidance data with final tracking including established orbital insertion conditions. Final tracking for most flights was not received in time to be used for the "Test Flight Results" analyses; therefore, intermediate tracking data were used to isolate any significant guidance system error greater than predictions based on laboratory tests of the hardware.

The general philosophy followed for the evaluation reports was to assume the error predictions were known error terms and then solve for a minimum of additional values required to approximate the velocity error profiles. For this report, the error predictions were used as "a priori" estimates and a more complete guidance error model was used with the best tracking data available for each vehicle flight. Although the final results are very similar, they are not necessarily identical to those shown in reports, "Results of the Saturn I Launch Vehicle Test Flight", published soon after each vehicle flight. (See References)

This report presents for each vehicle the velocity component errors versus time for the total powered flight, combinations of platform system errors that would produce the velocity error profiles, and the velocity component error corresponding to each platform system error.

(U) 2.0 SATURN I BLOCK II GUIDANCE SYSTEMS

The platform systems flown on the Saturn I Block II vehicles and the function of each system are shown in Table 2-1.

Although two previous vehicles, SA-3 and SA-4, carried prototypes of the ST-124 platform, Saturn SA-5 was the first vehicle to carry the complete ST-124 guidance system. Inertial velocities and vehicle attitudes referenced to the ST-124 platform were fed into an ASC-15 guidance computer for computations of "Path Adaptive" guidance commands and to initiate discreet signals. The guidance was in open loop.

An ST-90-S platform system was also carried on the SA-5 vehicle and used as a reference for attitude control. The ST-90-S platform was a modification of the ST-90 system flown on the Jupiter flights. The modification consisted of an extended azimuth drive to permit a programmed roll maneuver to turn the vehicle from a 90 degree launch azimuth to the desired flight azimuth.

[redacted]

Saturn SA-6 also carried two platform systems. The ST-90-S system generated signals to turn the vehicle into the desired flight azimuth and served as a reference for attitude control of the S-I stage. At about 14 sec after S-I/S-IV separation, attitude error signals were switched from the ST-90-S to the ST-124 platform. At about 168 sec of flight, the guidance loop was closed and the vehicle flew a guided trajectory, "Path Adaptive" in the pitch plane and "Delta Minimum" in the yaw plane, referenced to the ST-124 platform system.

Saturn SA-7 and subsequent Saturn I Block II vehicles carried only the ST-124 platform systems which generated signals to turn the vehicles into the desired flight azimuth and served as reference for attitude control of the S-I stages. The guidance loop was closed in the S-IV stage of each vehicle. SA-7 utilized the "Path Adaptive" and "Delta Minimum" guidance mode for pitch and yaw, respectively. SA-9, SA-8, and SA-10 vehicles utilized the "Iterative" guidance mode (IGM) and "Delta Minimum" for pitch and yaw, respectively.

The S-IV stage of each of the guided Saturn I Block II vehicles was guided to satisfactory orbital insertion conditions.

TABLE 2-I
SATURN I BLOCK II PLATFORM SYSTEMS

Vehicle	Platform System	Function
SA-5	ST-90-S	Initial roll maneuver and attitude control reference entire powered flight
	ST-124	Passenger
SA-6	ST-90-S	Initial roll maneuver and attitude control reference S-I stage
	ST-124	Attitude control and closed loop "Path Adaptive" guidance reference S-IV stage
SA-7	ST-124	Attitude control and closed loop "Path Adaptive" guidance reference entire powered flight
SA-9	ST-124	Attitude control and closed loop "Iterative" guidance reference entire powered flight
SA-8	ST-124	Attitude control and closed loop "Iterative" guidance reference entire powered flight
SA-10	ST-124	Attitude control and closed loop "Iterative" guidance reference entire powered flight

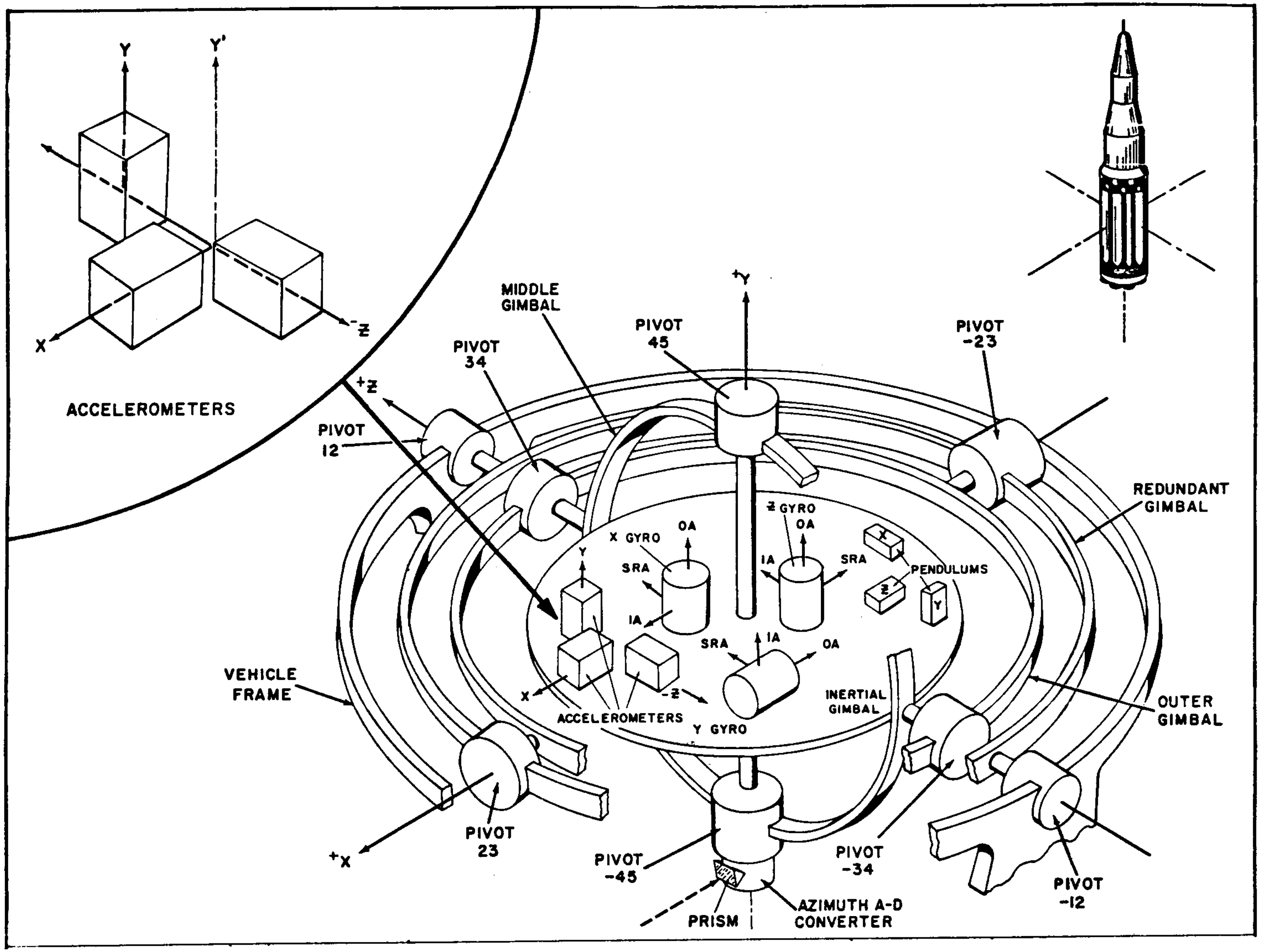

FIGURE 3-1 ST-124 PLATFORM SCHEMATIC

([redacted]) 3.0 DESCRIPTION OF THE ST-124 PLATFORM SYSTEM

The ST-124 platform is a four-gimbal system which permits full freedom about all three vehicle axes. The gimbal order from the vehicle to the inner gimbal is pitch redundant, yaw, pitch limited, and roll. The pitch redundant gimbal is positioned from a pitch command resolver and a gimbal resolver operating into an associated gimbal servo. The pitch limited gimbal is controlled to essentially zero (steady state).

Three pendulous integrating gyro accelerometers (AMAB-3-K4) are mounted on the ST-124 stabilized element. The range and cross range accelerometers are normal to each other in the local horizontal plane at launch with the range accelerometer directed down range. Cross range output is positive right with observer facing down range. The altitude accelerometer is directed up and normal to the launch horizontal plane.

The ST-124 platform is stabilized by three (AB-5-K3-P) air bearing, single-degree-of-freedom gyros mounted with the sensitive axes mutually perpendicular. The gyro axes (sensitive or input, output, spin reference) are oriented such that some of the "g"-sensitive drifts and all the "g2"-sensitive drifts are effectively zero or, in any case, a minimum. A schematic of the ST-124 platform system is shown in Figure 3-1.

([redacted]) 4.0 ERROR ANALYSES

The error analyses of the ST-124 guidance platform system are based on comparisons of the telemetered guidance velocities with final tracking data for each vehicle. Although the results are very similar, they are not necessarily identical to those presented in "Test Flight Results" published soon after each vehicle flight (see References).

The guidance error model used for the analyses has been simplified by combining error terms that produce like velocity error profiles and eliminating error terms that are generally considered negligible. Because of the alignment of the platform at launch with respect to the plane containing the thrust vector, some of the drifts caused by mass unbalance and all of the anisoelastic drifts are negligible.

The platform is leveled in the horizontal plane at launch with the cross range accelerometer electronically aligned in azimuth. Since the cross range acceleration is essentially zero during flight, an error component picked up by either the range or altitude accelerometers rotated into cross range would be negligible for small angle rotations. Thus, the altitude accelerometer error in the pitch plane usually is the only nonorthogonality error considered. A total of eighteen platform system error terms has been considered in the analyses. The error term considered are:

a. Bias error for each of the three accelerometers.
b. Scale factor error for range and altitude accelerometers. Scale factor error for cross range is negligible.
c. Nonorthogonality of altitude accelerometer in the pitch plane.
d. Initial platform alignment errors in pitch, yaw,and azimuth.
e. Constant drift of the platform about the input axes of the three stabilizing gyros.
f. "g"-sensitive drift due to mass unbalance along the spin reference axes of the yaw (X) and roll (Y) gyros.
g. "g"-sensitive drift due to mass unbalance along the input axis of the pitch (Z) gyro.
h. End plate "g"-sensitive turbine torque for each of the three stabilizing gyros.

The guidance platform error model is described by the following equation:

$$\overline{\Delta \ddot{X}} = \overline{B} + S\, \overline{\ddot{X}m}\, [M_{pq}]\, [\delta]\, \overline{\ddot{X}m}$$

where B = accelerometer bias error.

S = accelerometer scale factor error.

Subscript m = denotes an ideal measuring system.

$[M_{pq}]$ = 3 X 3 matrix defining the misalignment of the sensitive axis of the pth accelerometer about the qth axis.

$[\delta]$ = 3 X 3 matrix defining the instantaneous alignment of the platform with respect to the ideal alignment. This includes the effects of all drift terms.

Measurements made by the guidance accelerometers are referenced to a point in inertial space. This point coincides with the launch site at time of "Guidance Release" which occurs at or just prior to liftoff of the vehicle. Ideally, the stabilized platform on which the accelerometers are mounted remains fixed in inertial space throughout flight. Errors made in the velocity measurements result from imperfect accelerometers and nonideal alignment of the stable platform at any time after guidance release. In order to determine the platform system errors that were present during a vehicle flight, the measured velocities are referenced against a set of data that describes the trajectory of the particular flight.

The reference data used in these analyses vary from flight to flight according to the availability of precision tracking data. In each case the established insertion conditions were considered to be more accurate than data from any individual tracking system.

Tracking data, including established insertion points, are converted to the guidance coordinate system and compared with the guidance accelerometer outputs (guidance minus tracking) to establish the vehicle error profiles. Although tracking data contain errors peculiar to each tracking system, only random noise is considered in the covariance matrix used in the guidance error analysis. The tracking data have been processed to eliminate, to some extent, known errors before comparisons are made with guidance.

The guidance velocity error model is fitted to the velocity error profiles by a double precision weighted "Least Squares" method to determine a set of guidance system errors that would produce the velocity deviations (residuals) between the measured guidance data and tracking.

The general equation for the "Least Squares" solution is

$$\overline{U} = [\omega_o + P^T W P]^{-1} [\omega_o U_o + P^T W \overline{R}]$$

where $\overline{U}$ = platform system errors (n x 1)

P = 3 X n matrix of partial derivatives relating the velocity error to the platform system errors.

Superscript T = denotes matrix transpose.

Superscript -1 = denotes matrix inverse.

W = 3 X 3 covariance matrix associated with the residuals.

ω_o = n X n covariance matrix associated with the platform system error terms.

$\overline{R}$ = 3 X 1 matrix of residuals (Guidance minus Tracking).

U_o = n X 1 matrix of "a priori" estimates of the platform system error terms.

4.1 GUIDANCE VELOCITY COMPARISONS

The reference data used for guidance comparisons varied between flights. For the first three Saturn I Block II (SA-5, SA-6, SA-7) flights no tracking system adequately covered the major portion of the flight. Therefore, final postflight trajectories, based on various tracking and insertion data, were used for establishing the guidance velocity error profiles. MISTRAM, tied to close-in tracking from Cape Kennedy, and insertion data were used as reference data for vehicles SA-9 and SA-8. The analysis for SA-10 was based on ODOP tracking and insertion data. The quality of the tracking from the individual systems used for SA-9, SA-8, and SA-10 was verified by adjusting the measured guidance velocities for errors corresponding to the analyses made and computing trajectories that satisfied conditions established for orbital insertion of each vehicle. The velocity conditions were completely satisfied and position differences were within the accuracies associated with the insertion data.

The comparisons of the velocity components are shown, plotted versus range time, in Figures 4-1 through 4-6. The solid lines represent the comparisons between guidance velocities and range tracking or (for vehicle SA-5, SA-6, SA-7) final postflight trajectory. The circled points represent velocity differences associated with the guidance system errors determined from the analyses. The comparisons with established insertion velocities are shown enclosed in squares.

The inertial velocity components and total velocities at cutoff of the S-I stage and orbital insertion are shown for each vehicle in Table 4-I. Predicted, tracking, and telemetered values are shown for comparison. Since the Saturn vehicles are not constrained to a predetermined powered trajectory and the programmed S-IV cutoff velocity is in a space-fixed (includes the effect of gravity) plumbline coordinate systems, the telemetered inertial velocities are not necessarily close to predicted values. The velocity differences reflect the nonstandard performance of the total vehicle system in addition to any guidance errors.

The velocity differences between telemetry and tracking reflect the errors of the guidance system. Although tracking does contain errors, the values in Table 4-I should be valid especially at orbital insertion.

The inertial velocity outputs of the guidance accelerometers were converted to space-fixed values by the onboard (ASC-15) guidance computer for use in path guidance computations. Table 4-II shows the space-fixed velocities telemetered from the guidance computer compared with precalculated and orbital tracking at time of orbital insertion. Since SA-5 was flown with open loop guidance, this vehicle was not included.

[redacted]

(C) TABLE 4-1
INERTIAL VELOCITY COMPARISONS

Event	Range Velocity (m/s)			Altitude Velocity (m/s)			Cross Range Vel. (m/s)			Total Velocity (m/s)		
	Pred.	Track.	Telem.	Pred.	Track.	Telem.	Pred.	Track.	Telem.	Pred.	Track.	Telem.
O.E.C.O												
SA-5	2408.5	2444.8	2444.2	2658.0	2653.7	2655.2	- 1.1	- 35.3	- 35.6	3586.9	3603.4	3609.1
SA-6	2431.7	2356.8	2356.5	2509.5	2461.9	2464.4	- 6.6	- 6.3	- 6.9	3494.4	3408.2	3409.8
SA-7	2434.8	2457.0	2456.0	2522.1	2574.7	2575.2	- 8.4	- 14.1	- 11.3	3505.6	3558.9	3558.6
SA-9	2121.2	2128.9	2129.1	3048.7	3085.6	3085.7	-11.1	- 11.0	- 11.6	3714.1	3748.8	3749.0
SA-8	2186.8	2186.4	2186.3	3056.5	3078.2	3078.2	- 5.6	- 0.1	- 0.5	3758.2	3775.7	3775.6
SA-10	2193.0	2179.6	2179.8	3069.8	3087.1	3086.9	- 4.8	- 6.4	- 6.1	3772.7	3779.0	3778.9
Orbital Insertion												
SA-5	NA	7714.5	7713.5	NA	2961.2	2967.1	NA	-106.2	-105.1	NA	8264.0	8265.2
SA-6	NA	7642.7	7642.2	NA	3048.6	3055.9	NA	4.1	0.1	NA	8228.3	8230.5
SA-7	7629.9	7632.9	7631.9	2972.0	2967.4	2970.4	- 0.2	- 4.9	- 0.4	8188.3	8189.4	8189.6
SA-9	7492.6	7484.9	7485.8	3125.8	3074.7	3076.0	- 0.1	1.5	- 0.4	8118.5	8091.8	8093.1
SA-8	7485.2	7481.8	7482.0	3119.9	3089.7	3088.5	- 0.2	3.8	- 0.3	8109.4	8094.7	8094.4
SA-10	7402.5	7400.3	7400.4	3168.7	3147.5	3146.1	- 0.1	- 0.3	- 0.3	8052.2	8041.8	8041.4

NA = Not available

[redacted]

[redacted]

TABLE 4-11

(C) SPACE-FIXED VELOCITY COMPARISONS AT ORBITAL INSERTION

Parameter	Vehicle				
	SA-6	SA-7	SA-9	SA-8	SA-10
Total Velocity (m/s)					
Precalculated	7805.95	7807.5	7682.08	7675.18	7595.0
ASC-15 Computer	7812.2	7808.7	7682.15	7675.06	7594.9
Orbital Tracking	7811.8	7810.4	7681.82	7674.46	7594.3
Range Velocity (m/s)					
Precalculated	7288.7	7265.4	7235.58	7230.13	7157.7
ASC-15 Computer	7277.1	7260.8	7244.60	7233.68	7158.5
Orbital Tracking	7276.8	7261.6	7243.76	7233.23	7158.2
Altitude Velocity (m/s)					
Precalculated	-2793.5	-2857.3	-2579.39	-2574.09	-2539.6
ASC-15 Computer	-2840.5	-2872.0	-2554.13	-2564.44	-2537.4
Orbital Tracking	-2840.1	-2874.7	-2555.57	-2563.34	-2536.0
Cross Range Velocity (m/s)					
Precalculated	- 84.9	- 85.5	- 86.67	- 86.91	- 35.4
ASC-15 Computer	- 80.3	- 85.2	- 87.18	- 87.19	- 35.0
Orbital Tracking	- 80.8	- 89.4	- 85.64	- 83.41	- 35.4

[redacted]

[redacted]

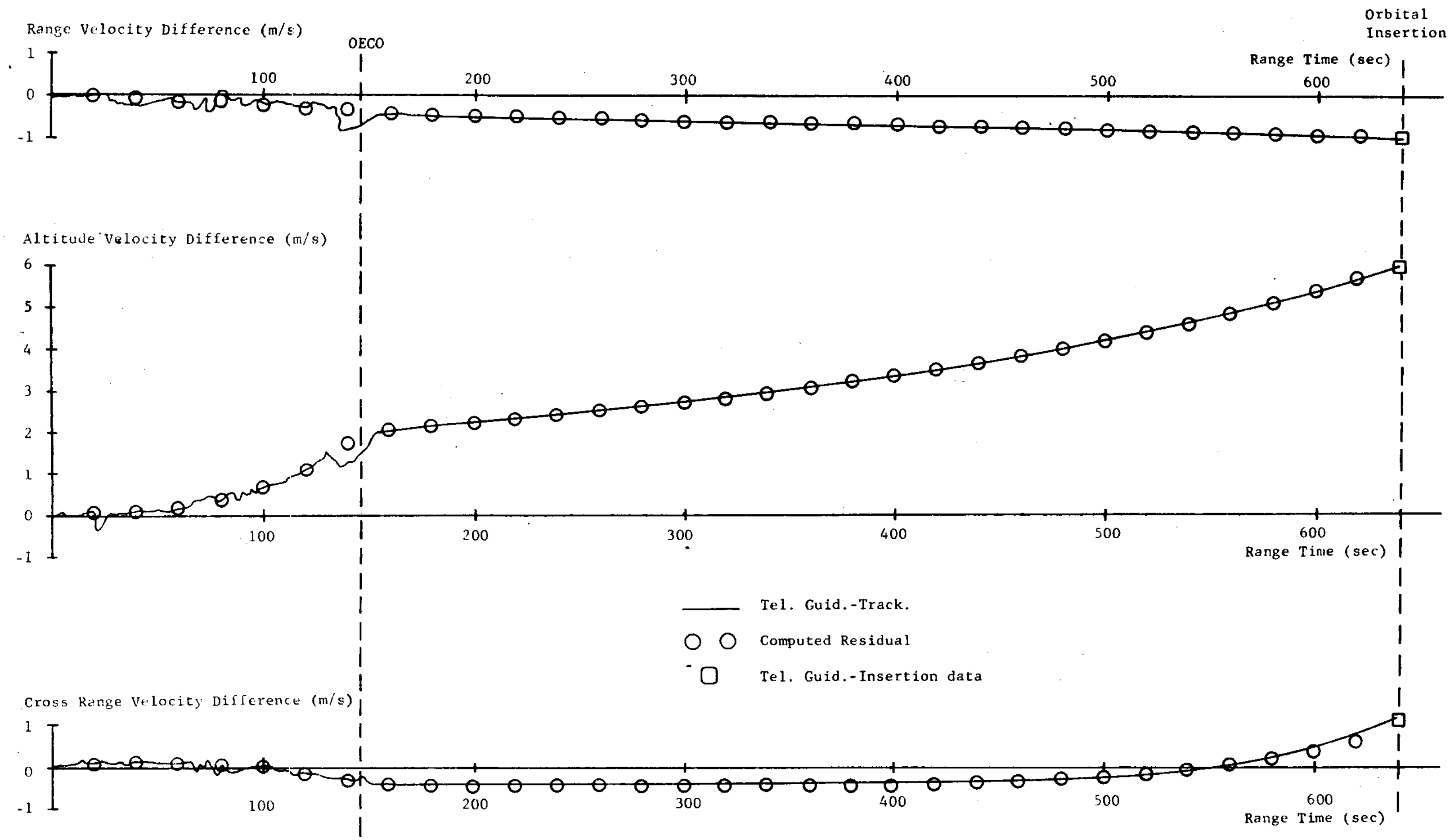

FIGURE 4-1 INERTIAL VELOCITY COMPARISONS SA-5 (TELEMETERED MINUS TRACKING)

[redacted]

[redacted]

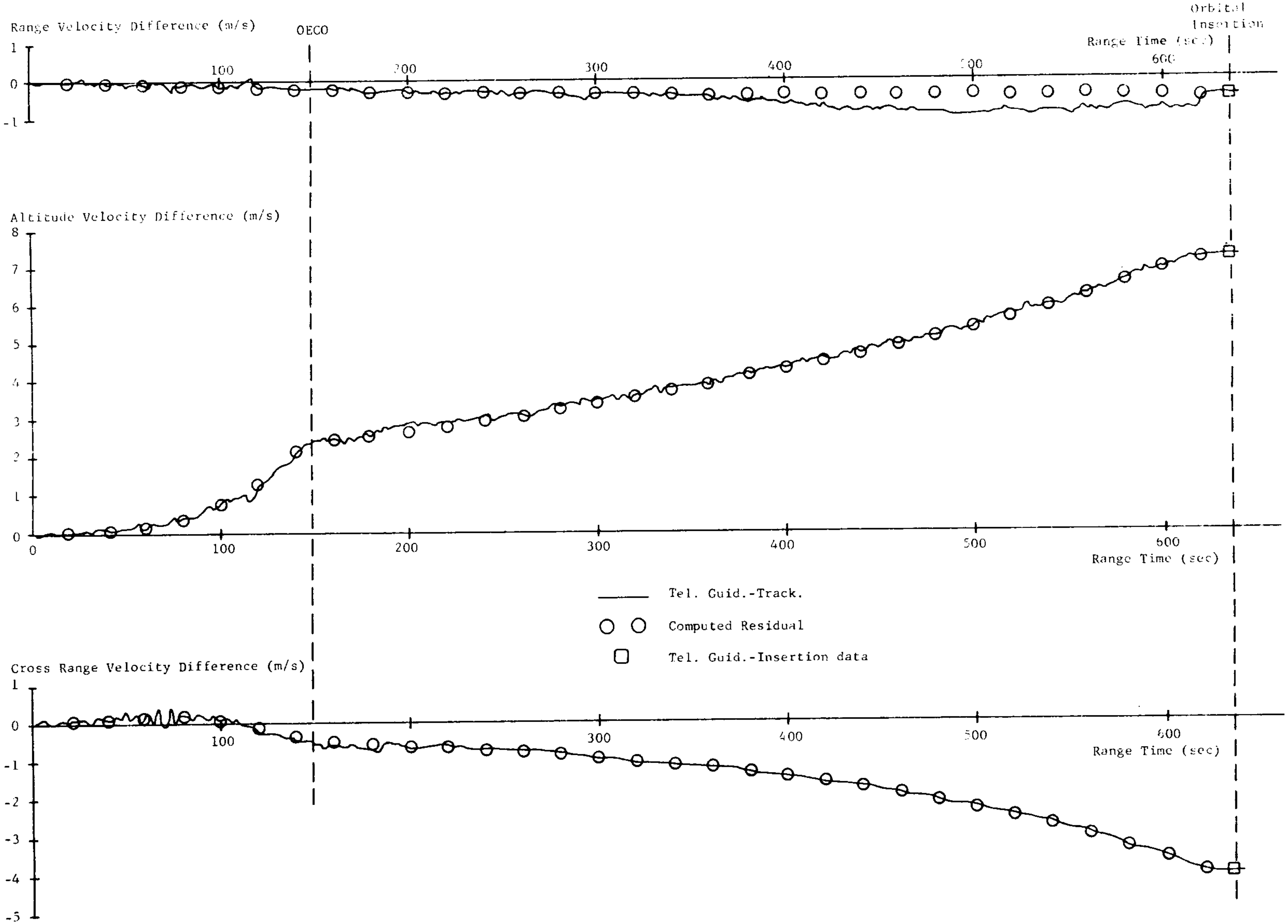

FIGURE 4-2 INERTIAL VELOCITY COMPARISONS SA-6 (TELEMETERED MINUS TRACKING)

[redacted]

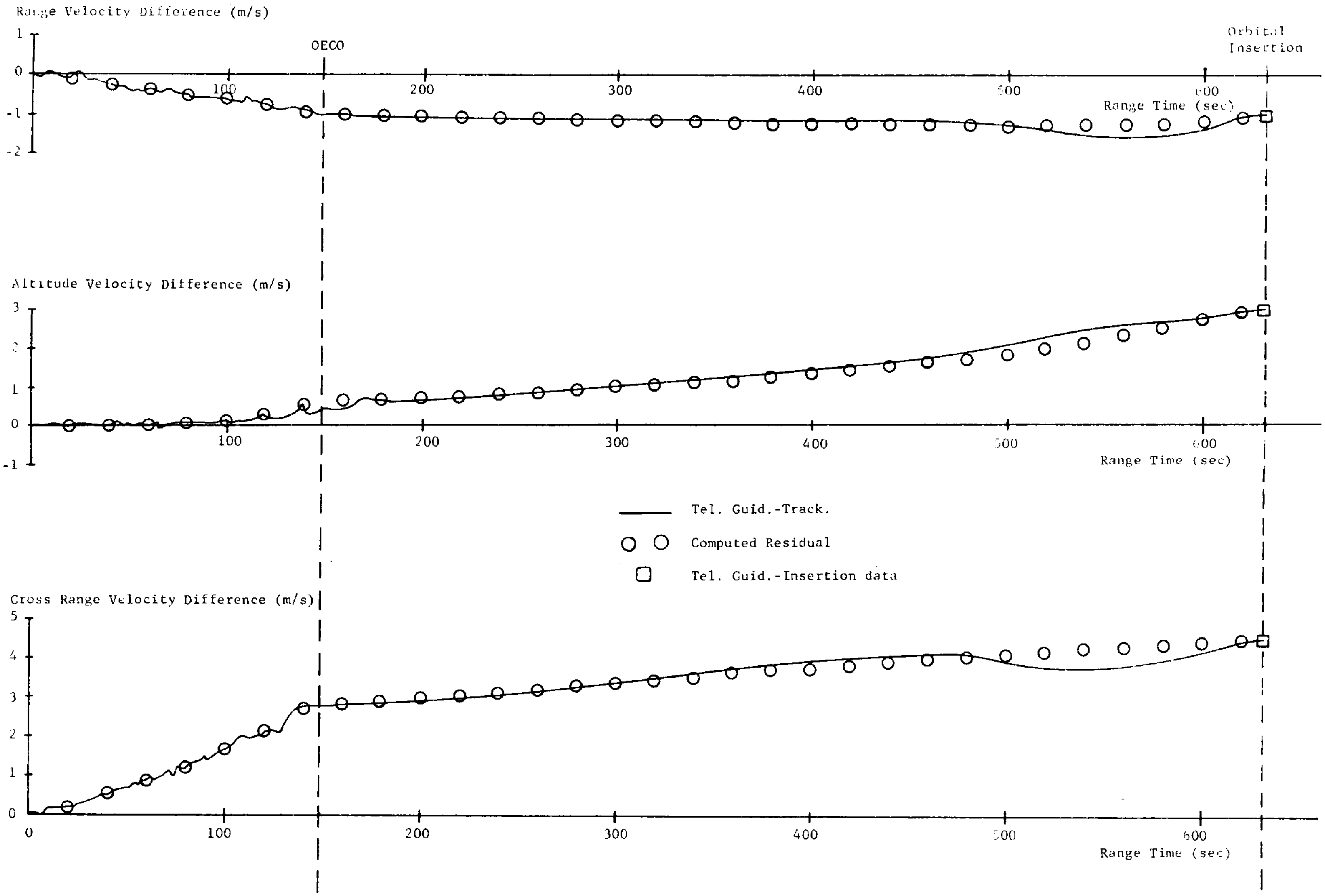

FIGURE 4-3 INERTIAL VELOCITY COMPARISONS SA-7 (TELEMETERED MINUS TRACKING)

[redacted]

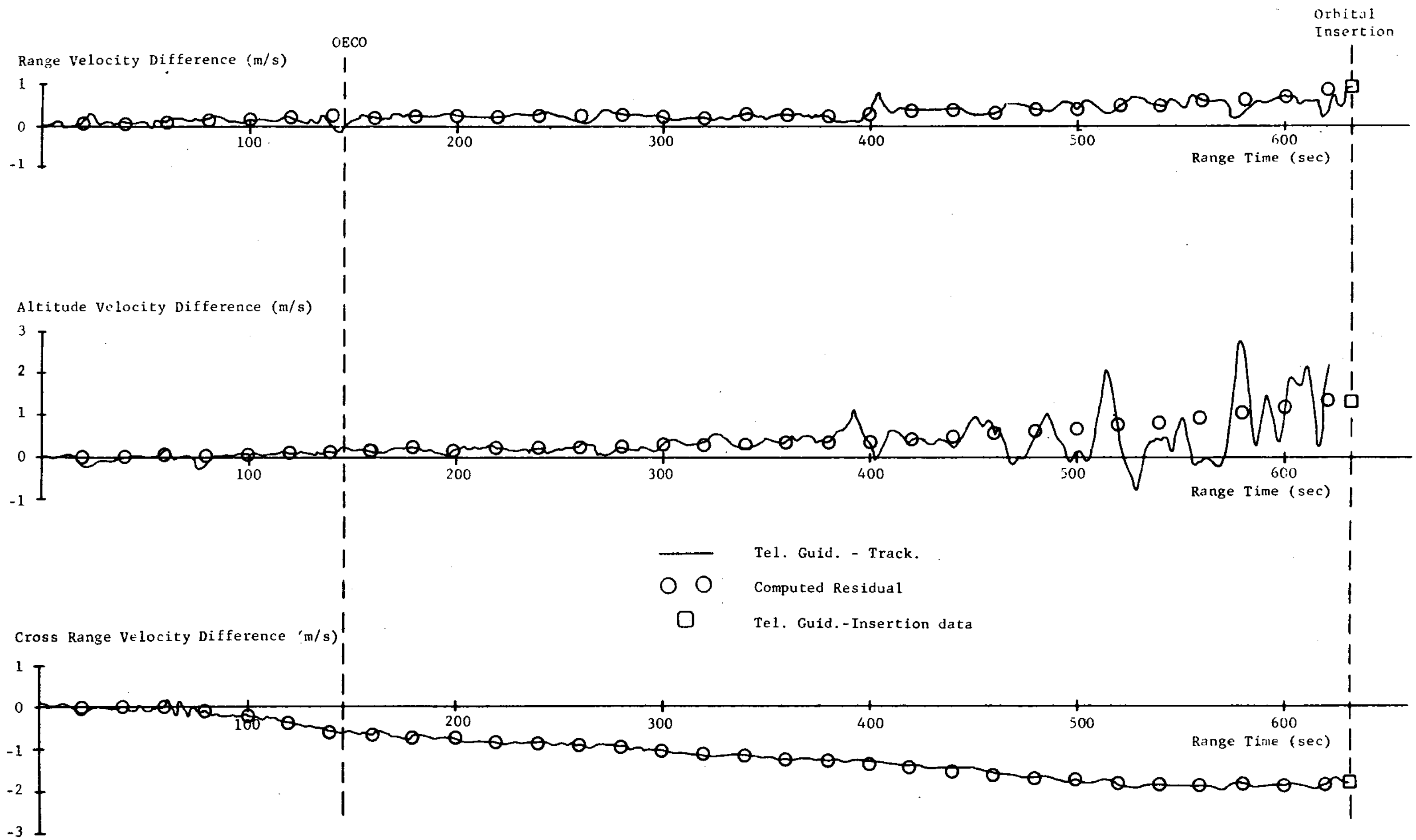

FIGURE 4-4 INERTIAL VELOCITY COMPARISONS SA-9 (TELEMETERED MINUS TRACKING)

[redacted]

[redacted]

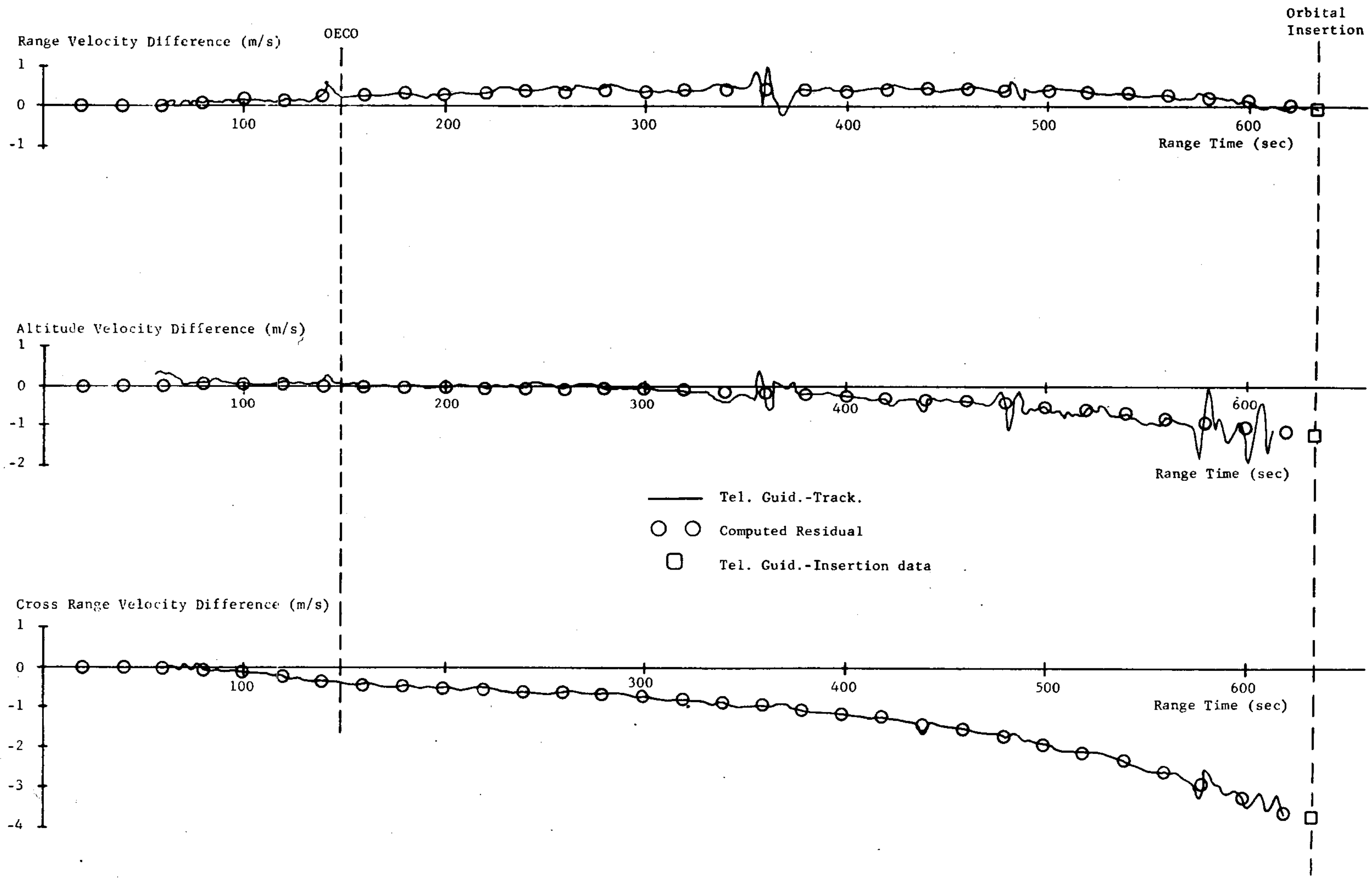

FIGURE 4-5 INERTIAL VELOCITY COMPARISONS SA-8 (TELEMETERED MINUS TRACKING)

[redacted]

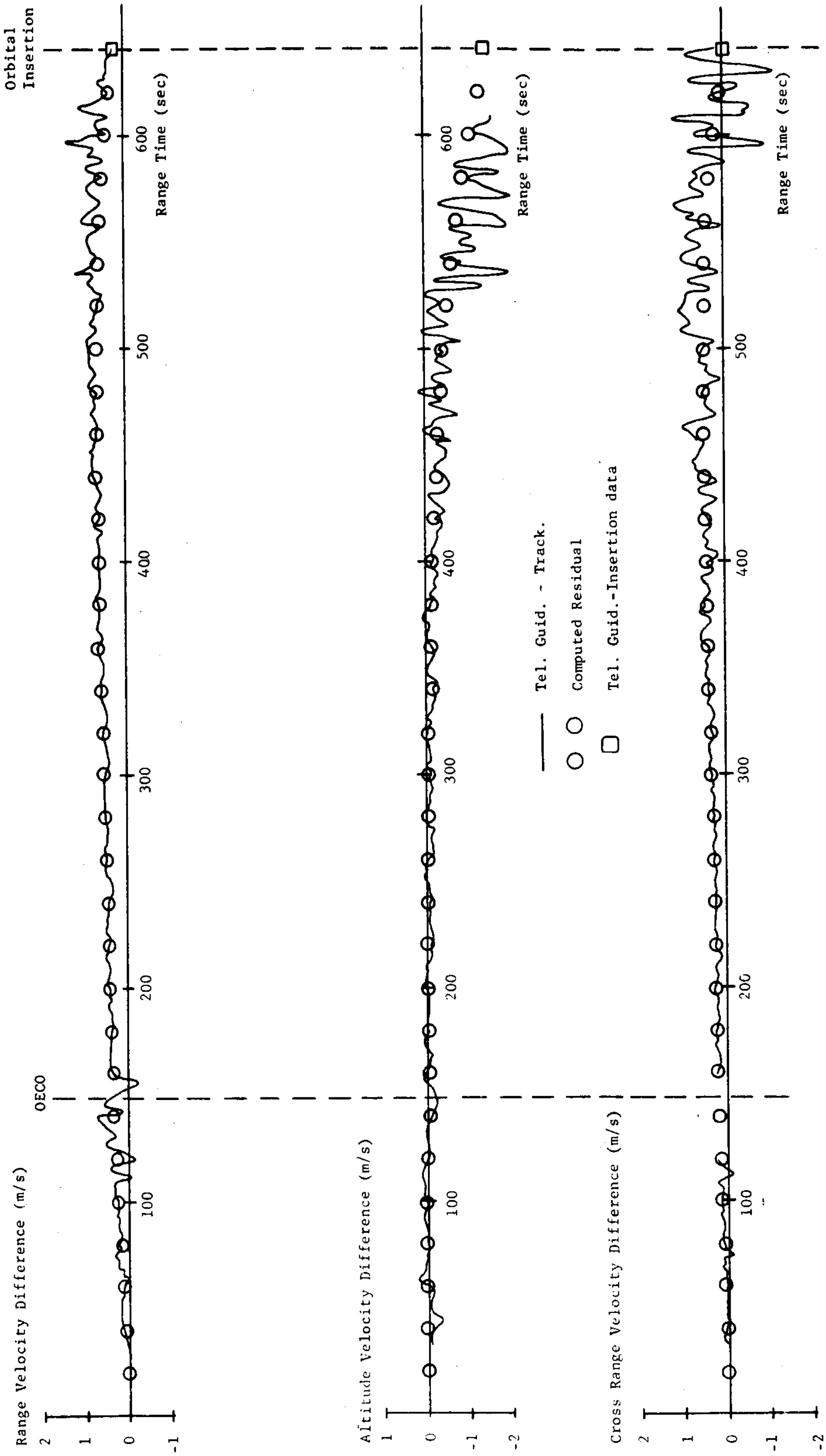

FIGURE 4-6 INERTIAL VELOCITY COMPARISON SA-10 (TELEMETERED MINUS TRACKING)

The precalculated velocity vector at S-IV cutoff was preset in the guidance computer and cutoff signal was issued when the onboard measurement equaled the preset value. Orbital insertion occurred 10 sec after S-IV cutoff. For SA-6 the precalculated velocity vector at insertion was erroneously preset in the guidance computer as cutoff velocity which explains most of the 6.2 m/s velocity difference at insertion. For vehicles SA-6 and SA-7 the time delay between cutoff signal and actual cutoff was not included in computations of velocity increase due to thrust decay. This was included for subsequent vehicles and the deviation between the telemetered and precalculated velocity vectors was within ± 0.1 m/s at orbital insertion.

The differences between the telemetered guidance values and orbital tracking reflect the errors of the guidance system and errors in the gravity profiles based on the measured guidance velocities.

4.2 ST-124 PLATFORM SYSTEM ERRORS

The philosophy followed for the final analyses was that the most probable set of guidance errors would represent adjustments to the telemetered velocities necessary to simulate the vehicle trajectory with special emphasis on the orbital insertion conditions. Different philosophies concerning confidence in preflight estimates and predicted performance can vary solutions using the same data and method. This may be verified by comparing error solutions shown in Table 4-III. Essentially, the same method, weighted "Least Squares", was used for the postflight evaluation reports[1] as was used for the final analysis. The final tracking data was also available for SA-8 and SA-10 vehicles before the postflight evaluation reports were published. For the analyses used in these reports, the preflight estimates were considered generally accurate and weighted accordingly. A minimum amount of flexibility was permitted to give a solution that would fit the end point and given an error profile similar to the observed velocity differences. The solutions were constrained to the preflight estimates within the data noise level permitting a minimum of terms to exceed the preflight estimates.

The procedure used for the final analyses also utilizes a weighted "Least Squares" approach. However, preflight estimates of the error terms were used as "a priori" estimates for a first pass at fitting the established velocity error profiles. The only preflight errors weighted heavier than $\pm 3\sigma$ limits were the angular errors made in mounting the accelerometers on the platform (generally 0.1 times 3σ values). These are referred to as nonorthogonality of the individual accelerometer sensitive axis with respect to another accelerometer. Constraints were placed on the solution to insure a curve fit of the residuals to fall within the noise level of the data used. Completely wild data or data gaps were weighted out of the solution. Orbital insertion data were heavily weighted.

(1) Reports published by Flight Evaluation Working Group (See References).

Successive cases were computed, iterating around the previous case to eliminate unnecessary compensating error terms, until a set of guidance error terms was derived with a minimum number exceeding the magnitude of the "a priori" estimates and yet fit the observed velocity error curves. The solutions were verified as reasonable by adjusting the measured guidance velocities by the error solutions and computing trajectories that compared very favorably with the postflight trajectories and satisfied the insertion velocity components within ± 0.1 m/s and positions to within the accuracies quoted for the insertion parameter solutions.

Table 4-III presents the final platform system error solutions for each of the Saturn I Block II vehicles. Also shown for each vehicle are the preflight estimates of the errors and the values presented in the individual evaluation reports. The errors are listed under seven major types. Three types of errors, bias, scale factor, and nonorthogonality, pertain to the accelerometers. Two types, platform leveling in pitch and yaw and azimuth alignment, pertain to the orientation of the measuring directions at launch. Two types of drift, constant and "g"-sensitive. pertain to the stabilizing gyros. Although errors other than those listed are known to exist, they are either insignificant or cannot be distinguished from some one of the listed terms.

Since the acceleration in the cross range direction is very small or essentially zero for the major portion of powered flight, the scale factor errors of the cross range accelerometer and the nonorthogonality of the range and altitude sensitive axes with respect to the cross range direction were assumed to be as predicted. Any postflight solution for these errors would be highly questionable. For the same reason one "g"-sensitive drift term for each gyro and all anisoelastic drifts were not considered.

The final postflight analyses indicated the accelerometer bias errors were generally close to the preflight estimate. Of eighteen values (three accelerometers for each of six vehicles) fourteen were equal in sign or essentially zero. Only two accelerometers, range and altitude for SA-5 and SA-10 respectively, experienced bias errors significantly greater than the 3σ value of 0.5×10^{-3} m/sec^2.

The scale factor errors were essentially as predicted except for SA-9. The postflight solutions showed four values of different signs but essentially the same magnitude as predicted. This discrepancy could very well be due to interpretation of test data. The scale factor errors shown for SA-9 could be due to approximately 4 degree lower than normal gimbal temperature that was experienced in flight. Preflight estimates were assumed for the cross range accelerometer.

The platform is oriented so that the sensitive axes of the range and cross range accelerometers are in the horizontal plane with the cross range axis more accurately aligned. This procedure minimizes the range and azimuth errors leaving the nonorthogonality of the altitude accelerometer with respect to range direction the only effective error in mounting the accelerometers. Although the postflight solutions indicated the preflight measurements were highly accurate (less than 2 sec of arc except for SA-6 which was only 6.8 arc sec.), the accelerometer mounting was rather poor for SA-5 and SA-6. SA-7 was much more accurately assembled, but subsequent vehicles show that the accelerometers can be mounted to a high degree of precision.

The rather large leveling and azimuth errors noted on the first three Saturn I Block II vehicles were evidently due to vibrations during thrust buildup. The platform was torqued to compensate for earth's rotation until liftoff signal. When the platform became space-fixed at liftoff, the position of the platform became the gyro null position. The gyros stabilized the platform to the liftoff position. Beginning with SA-9, the platform was space-fixed prior to ignition and the initial errors were reduced to less than 3σ values in each case except for pitch leveling on SA-10 which was only 0.007 deg compared to the 3σ value of 0.005 deg. Leveling and azimuth preflight estimates shown are 3σ values.

With one exception the directions assigned to the preflight estimates of the guidance error terms shown in Table 4-III were taken from memoranda published prior to launch of each vehicle. In these memoranda nonorthogonality was defined as positive when the angle between the measuring directions of two accelerometers was greater than 90 degrees. In the analysis program the orthogonality error is considered as an angular rotation of the measuring direction about an axis and positive for a right hand rotation.

A positive bias of scale factor error indicates an accelerometer output greater than the absolute value. A positive platform alignment or gyro drift error permits the platform to move in a right-handed sense about the ideal axes and the vehicle follows the platform.

The predictions of the magnitude of the constant gyro drift terms were relatively consistent with the postflight results. Only three terms (X and Y gyros for SA-5 and Y gyro for SA-6)were significantly greater than predicted and one of the three (X gyro SA-5) was essentially a 3σ value of 0.075 deg/hr.

Gyro drifts referred to as "g"-sensitive drifts are due to mass unbalance along the input and spin-reference axes and end plate misalignment producing a torque proportional to acceleration parallel to the output axis. Since either the input or spin-reference axis is in the cross range direction for each gyro, only two "g"-sensitive terms for each gyro were considered. No predictions were published for the "g"-sensitive drifts on vehicles SA-5 and SA-6.

Several tests are made in the laboratory to approximate the "g"-sensitive gyro drifts. An average of these test results is published as the preflight estimate. These estimates are believed to be the least accurate of the predicted hardware errors due to inconsistency (non-repeatability) of day to day laboratory measurements. However, this should not be interpreted as a reflection on the quality of the gyros used with the ST-124 platform system. The drifts determined in the laboratory or from postflight analyses are probably within the accuracy of the measurements of other types of gyros that are less accurate but said to be more predictable.

The "g"-sensitive drifts determined from the postflight analyses closely agreed in magnitude with predictions for eighteen of the twenty-four terms shown. Of the remaining six terms that were significantly different in magnitude, four were much smaller.

The significance of the computed guidance error terms shown in Table 4-III is presented in Figures 4-7 through 4-12. The velocity error contribution for each hardware error was computed by multiplication of the respective partial derivatives times the error solutions. Delta velocities are shown at outboard engine cutoff, 350 sec, and S-IV stage cutoff for each vehicle. The time of 350 seconds was chosen for convenience as an approximate midpoint to give an indication of the velocity error buildup. Total velocity errors shown for each point correspond to respective points on curves presented in Figure 4-1 through 4-6.

Figures 4-7, 4-8, and 4-9 are of somewhat special interest. These Figures show the effects of the error solutions for SA-5, SA-6, and SA-7, respectively. For vehicles SA-5 and SA-6 it was not difficult to approximate the velocity error profile, as was done in the Evaluation Reports, with only one error exceeding the predicted values. Any deviation from the observed velocity error profile could be within the data noise level especially for preliminary data. However, it would seem more realistic, when using final comparison data, to permit more freedome of error distribution and fit the established error profiles. The solutions shown in Table 4-III for the final analyses would produce the observed velocity error profiles as shown in Figures 4-1 through 4-6.

Figure 4-9 shows for SA-7 the velocity errors associated with the hardware error solution. SA-7 velocity errors were expected to be much smaller than for the two previous flights. However, this was not the case. All attempts to get an unbiased postflight error solution indicated rather large leveling and azimuth error. Eventually, these misalignment errors were found to be due to vibrations during thrust buildup causing the platform to be stabilized at an erroneous position at liftoff signal when it became space-fixed. As a result, for subsequent vehicles the platform was space-fixed prior to ignition and any movement due to vibrations was sensed by the stabilizing gyros and corrected.

[redacted]

TABLE 4-III

(C) ST-124 PLATFORM SYSTEM ERRORS

Guidance Error / Vehicle Analysis	Bias ($m/s^2 X 10^{-3}$)			Scale Factor ($g/g X 10^{-4}$)			Nonorthogonality ($deg X 10^{-2}$)			Leveling ($deg X 10^{-2}$)		Azimuth ($Deg X 10^{-2}$)	Constant Drift (deg/hr)			"g"-sensitive drift (deg/hr/g)					
	Range	Altitude	Cross Range	Range	Altitude	Cross Range	Y to X	Y to Z	X to Z	δ_x	δ_z	δ_y	$\dot{\delta}_x$	$\dot{\delta}_y$	$\dot{\delta}_z$	$\dot{\delta}_{x/\ddot{x}}$	$\dot{\delta}_{x/\ddot{y}}$	$\dot{\delta}_{y/\ddot{x}}$	$\dot{\delta}_{y/\ddot{y}}$	$\dot{\delta}_{z/\ddot{x}}$	$\dot{\delta}_{z/\ddot{y}}$
SA-5: Preflt Est.	- .33	-.231	-.23	-.33	.39	.36	-3.97	-1.19	.56	± .5	± .5	±1.0	.006	-.014	-.008	NA	NA	NA	NA	NA	NA
Eval Rept.	-3.7	-.231	-.23	-.33	.39	.36	-3.97	-1.19	.56		- .4		.006	-.014	-.014						
Final Anal.	- .725	-.257	-.108	-.313	.423	.36	-3.92	-1.19	.56	-1.06	- .64	-2.54	.082	.17	.045	.043	.024	.099	.02	-.015	.015
SA-6: Preflt Est.	- .20	-.17	.033	.33	.099	.16	-5.69	-2.2	0	± .5	± .5	±1.0	.13	-.038	.053	NA	NA	NA	NA	NA	NA
Eval Rept	- .20	-.17	.033	.33	.099	.16	-5.69	-2.2	0	-2.6	- .5	-3.51	.13	-.038	.053						
Final Anal.	- .16	-.19	.29	-.33	-.25	.16	-5.50	-2.2	0	-1.15	- .42	-1.55	.11	-.15	.056	-.013	-.005	-.043	-.014	-.008	-.013
SA-7: Preflt Est.	- .63	0	-.56	.16	0	.29	.75	2.8	-.3	± .5	± .5	±1.0	.05	.03	.09	-.15	-.01	-.01	-.02	-.10	0
Eval. Rept	- .624	0	-.56	.164	0	0	.74	2.8	-.3	-5.1	-2.4	1.5	.05	.03	.09	-.15	-.01	-.01	-.02	-.10	0
Final Anal.	- .097	-.35	-.49	.31	-.23	.29	.75	2.8	-.3	-5.4	-2.25	1.2	.066	.07	.055	-.125	.004	-.006	-.042	-.14	.01
SA-9: Preflt Est.	.36	.066	-.20	.16*	.099*	.33*	-.04	- .33	-.31	± .5	± .5	±1.0	.164	-.041	-.024	.174	-.015	.05	.015	-.067	.025
Eval Rept.	.80	.02	-.22	.45	.06	0	-.04	- .33	-.31	.37	.22	.46	.135	.105	0	.165	-.031	.009	-.086	-.090	-.030
Final Anal.	.04	-.44	.13	.75	.72	.33	-.04	- .33	-.31	- .038	.35	-.65	.13	-.081	.027	.152	-.034	.03	-.048	-.166	.011
SA-8: Preflt Est.	0	.155	-.445	.132	.031	.264	-.292	- .067	-.40	± .5	± .5	±1.0	-.063	.060	.057	-.146	-.032	.072	.208	.177	.035
Eval Rept.	0	.262	-.527	.211	.307	.264	-.29	- .067	-.40	.09	.17	- .12	-.072	.036	-.027	-.171	-.006	-.08	-.22	.135	.006
Final Anal.	- .201	.555	-.408	-.102	.321	.264	-.292	- .067	-.40	- .10	.162	- .488	-.039	-.058	.055	-.156	.020	-.028	-.141	.036	.055
SA-10: Preflt Est	- .23	-.046	-.42	-.084	.13	.29	-.186	.214	.294	± .5	± .5	±1.0	.23	.138	.125	.241	-.0865	-.111	-.0455	.101	.049
Eval Rept.	.17	.89	-.007	-.024	.139	.29	-.186	.214	.294	.21	.68	-.096	-.086	.054	.11	-.10	-.047	-.107	.076	.046	-.06
Final Anal.	.52	.74	-.16	-.126	-.038	.29	-.193	.214	.294	-.169	.697	.091	-.226	.139	.112	-.043	.086	-.096	-.028	.094	-.121

* Due to approximately 4 degree lower than normal inertial gimbal temperature, postflight estimate of scale factor error was .768 X 10^{-4} g/g.

[redacted]

[redacted]

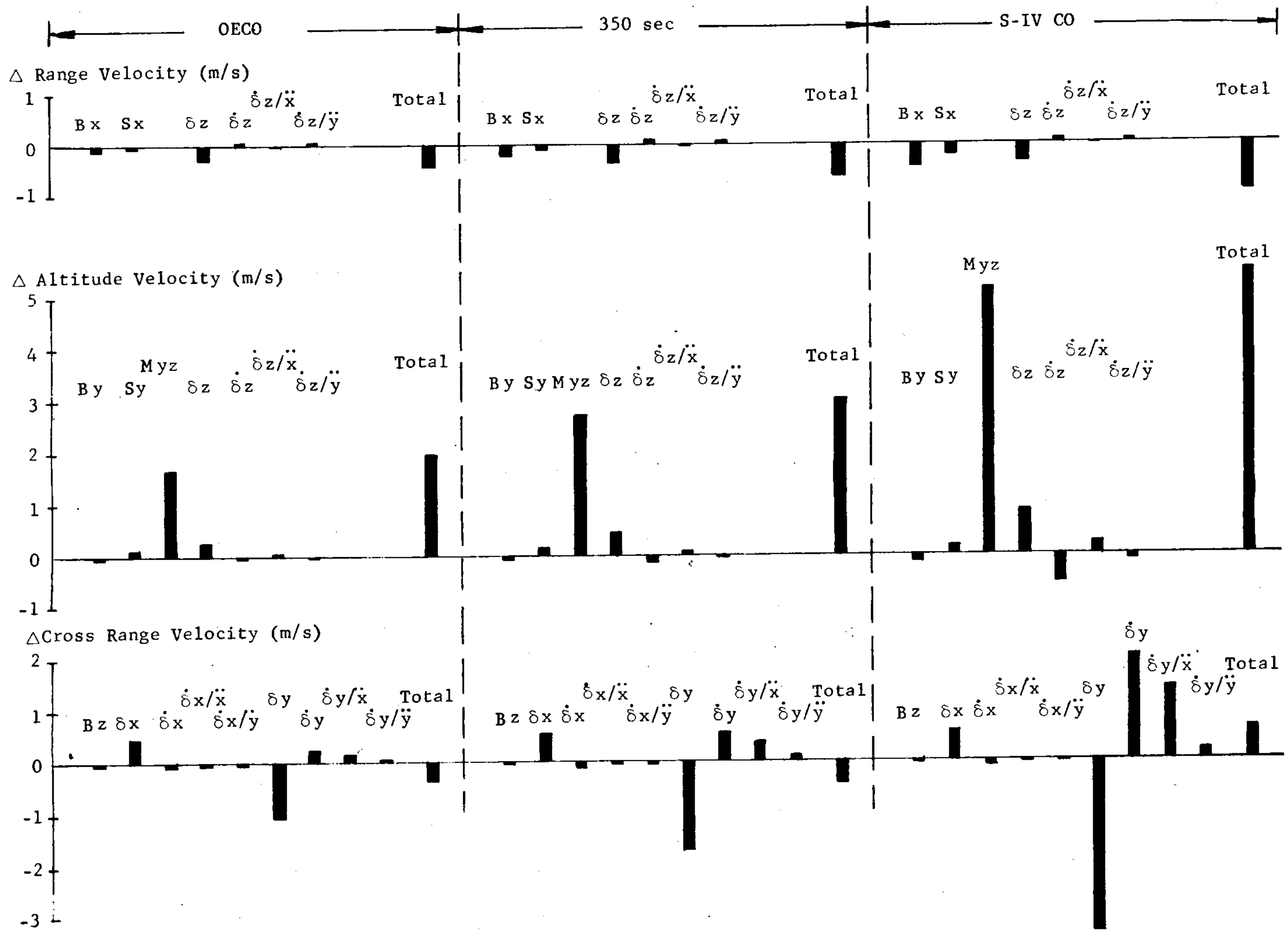

FIGURE 4-7 GUIDANCE HARDWARE ERROR CONTRIBUTION SA-5

[redacted]

[redacted]

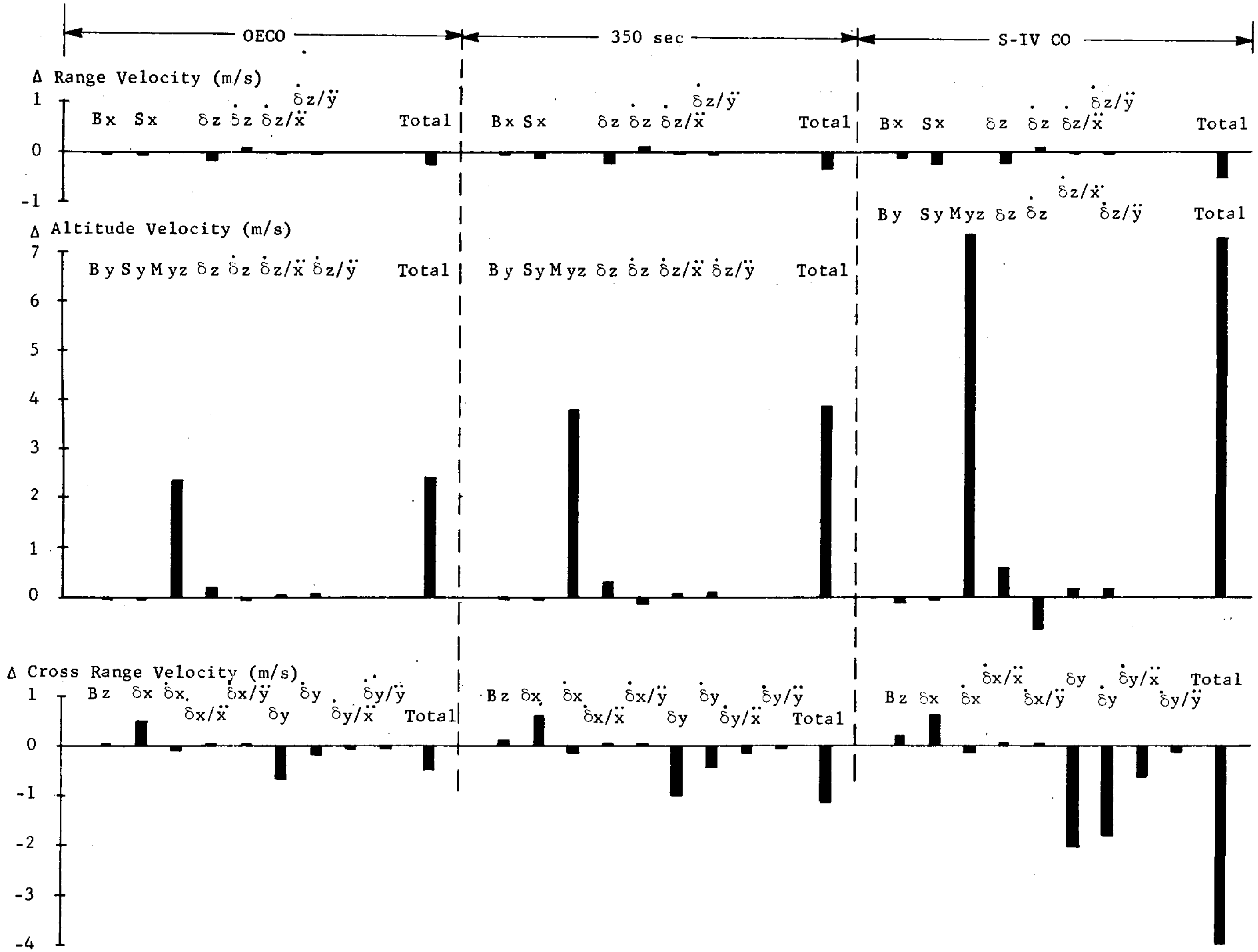

FIGURE 4-8 GUIDANCE HARDWARE ERROR CONTRIBUTION SA-6

[redacted]

[redacted]

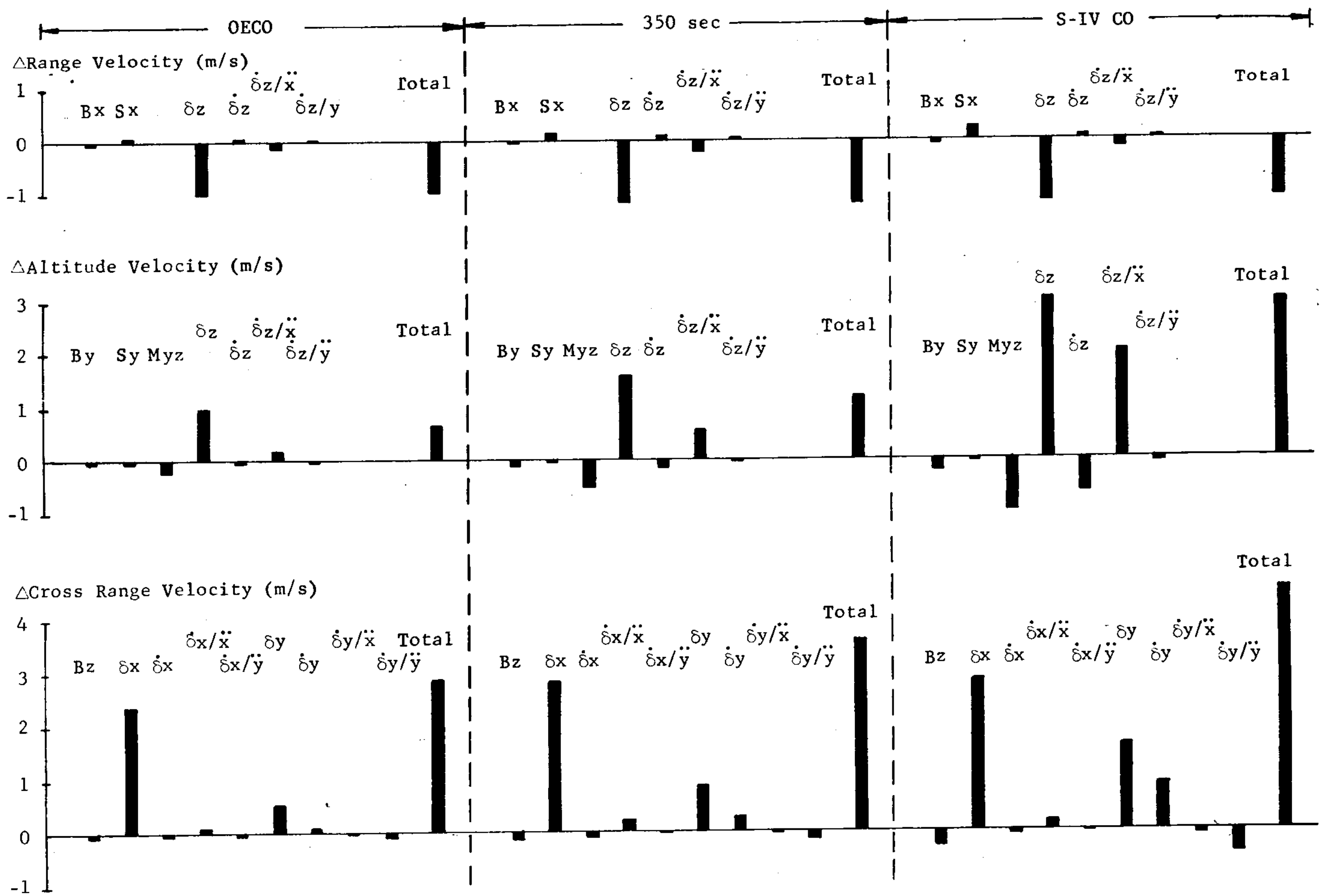

FIGURE 4-9 GUIDANCE HARDWARE ERROR CONTRIBUTION SA-7

[redacted]

[redacted]

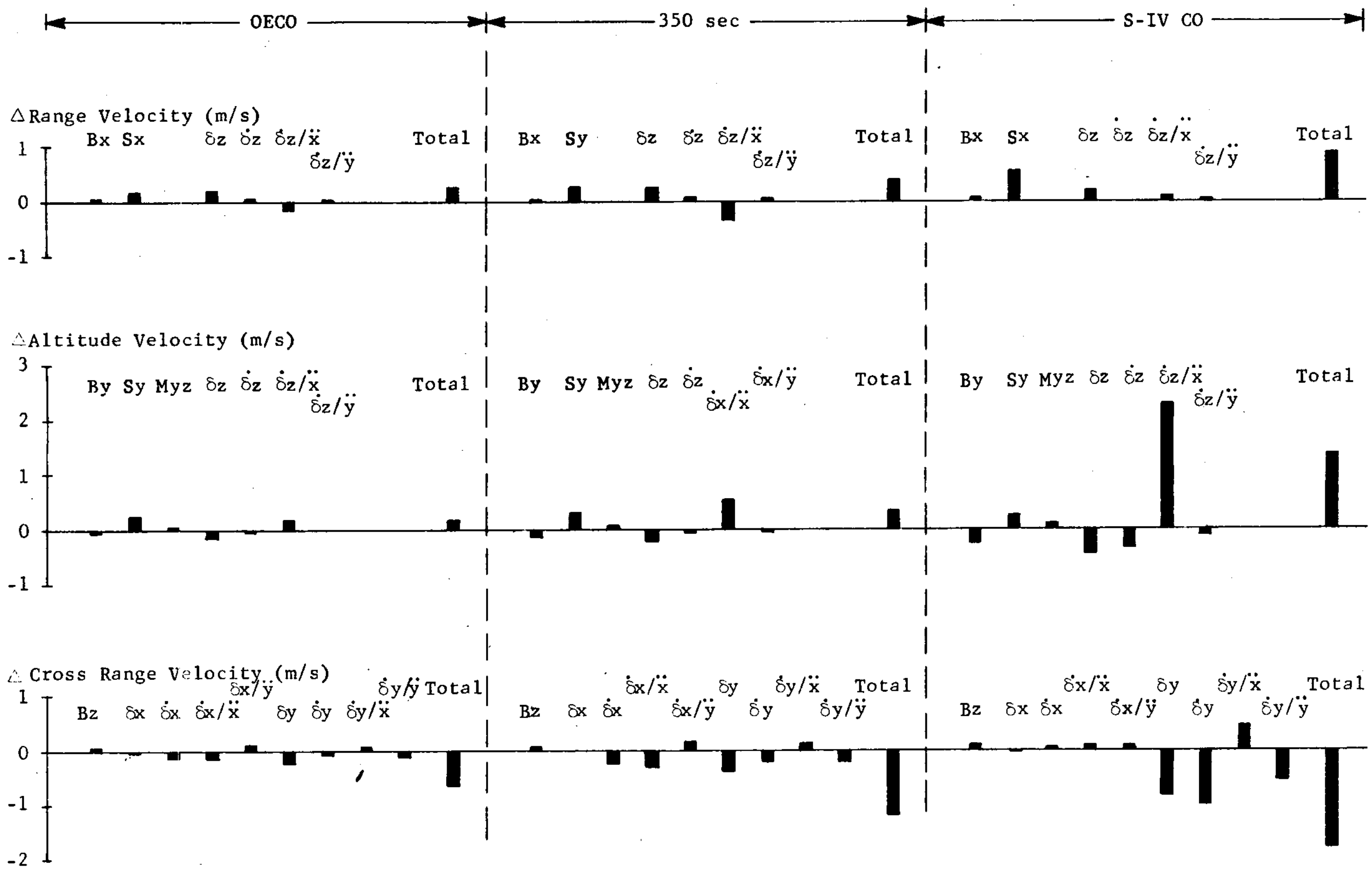

FIGURE 4-10 GUIDANCE HARDWARE ERROR CONTRIBUTION SA-9

[redacted]

[redacted]

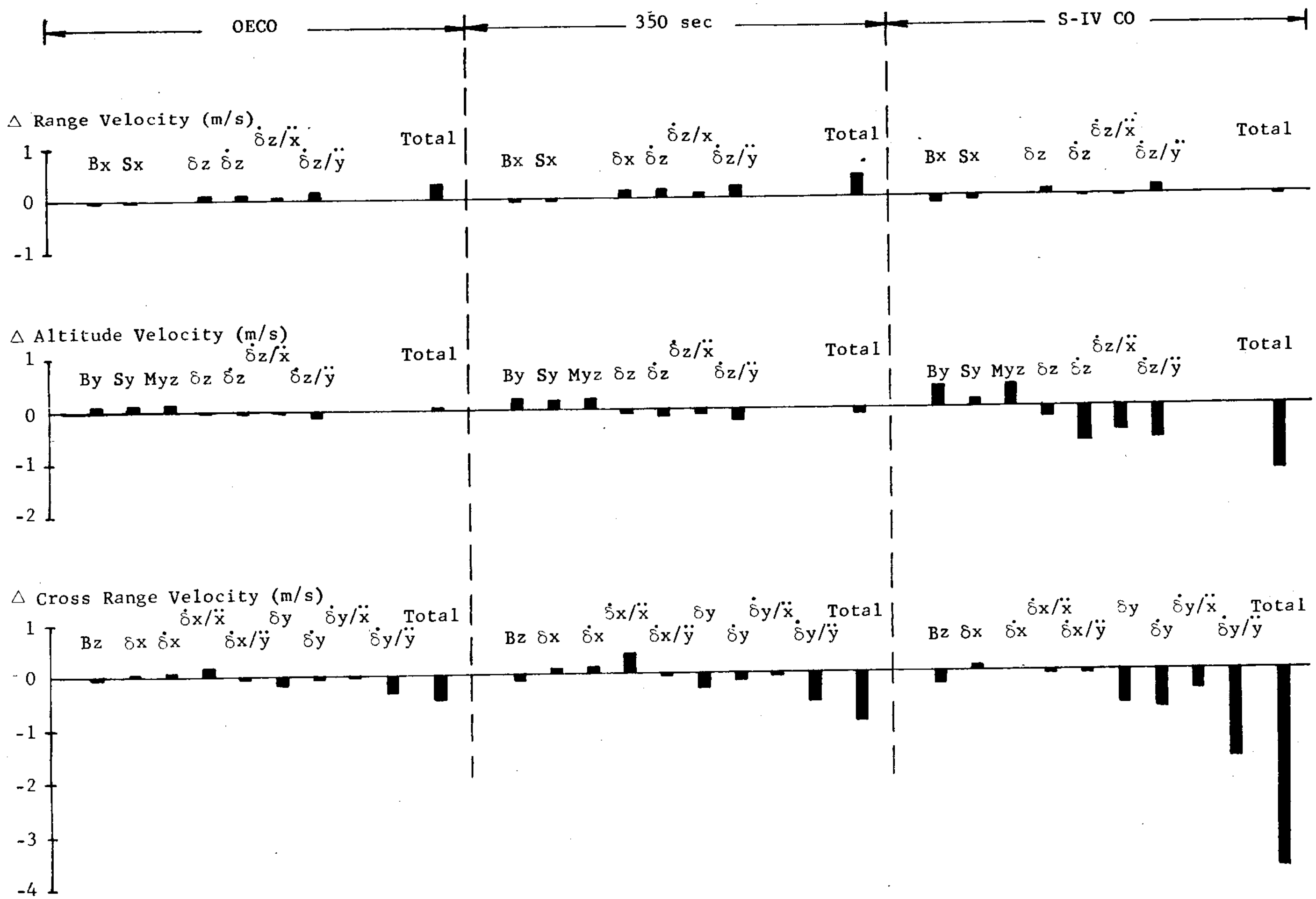

FIGURE 4-11 GUIDANCE HARDWARE ERROR CONTRIBUTION SA-8

[redacted]

[redacted]

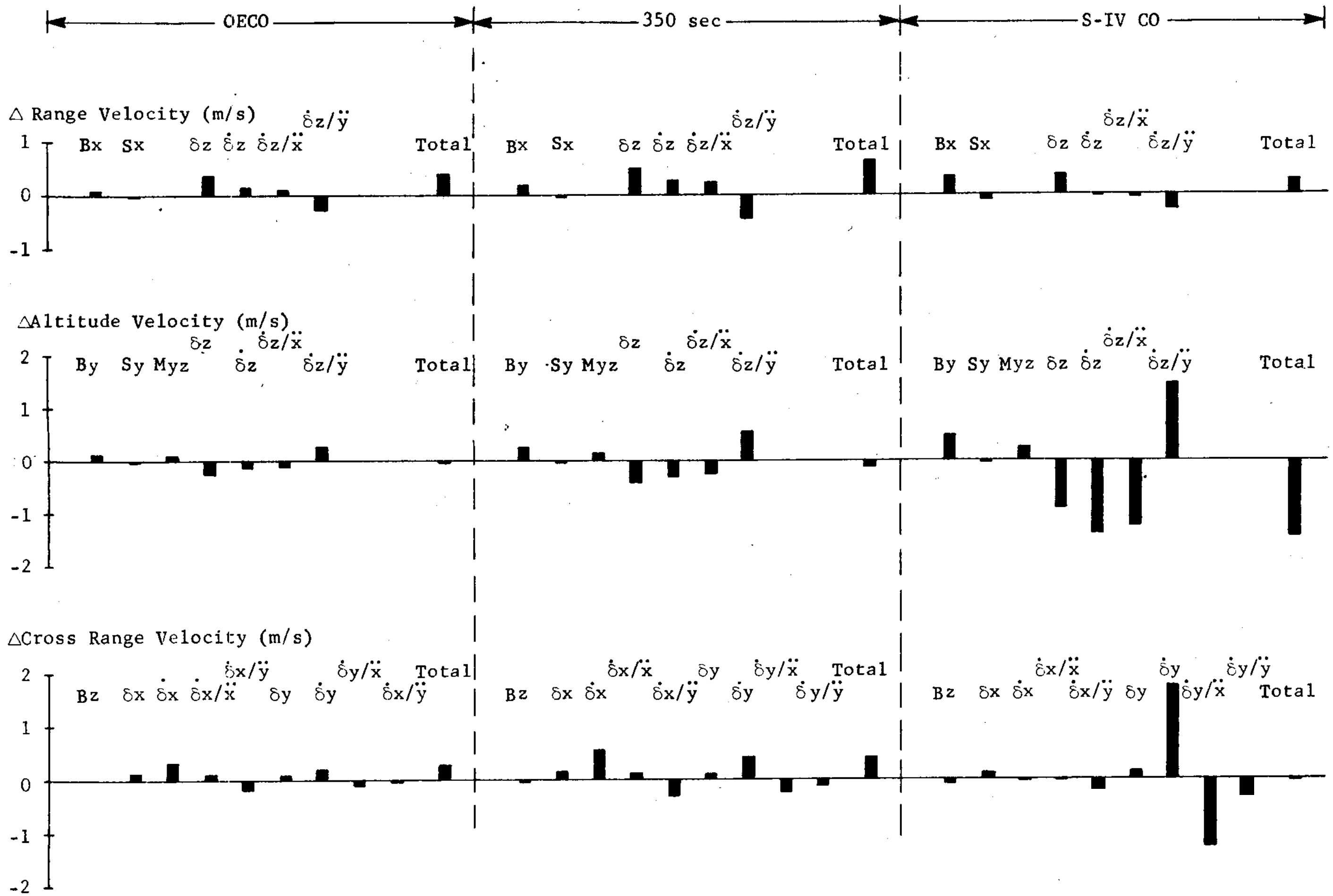

FIGURE 4-12 GUIDANCE HARDWARE ERROR CONTRIBUTION SA-10

[redacted]

TABLE 4-IV
CORRELATION COEFFICIENTS
$\rho_{ij} = \sigma_{ij}/\sigma_i\sigma_j$

i \ j	B_x	B_y	B_z	S_x	S_y	M_{yz}	δ_x	δ_y	δ_z	$\dot\delta_x$	$\dot\delta_y$	$\dot\delta_z$	$\dot\delta_{x/\ddot x}$	$\dot\delta_{y/\ddot x}$	$\dot\delta_{z/\ddot x}$	$\dot\delta_{x/\ddot y}$	$\dot\delta_{y/\ddot y}$	$\dot\delta_{z/\ddot y}$
B_x	1.	.2	0	.9	0	0	0	0	0	0	0	.1	0	0	.1	0	0	.1
B_y		1.	0	.2	.7	.5	0	0	.6	0	0	.3	0	0	.2	0	0	.3
B_z			1.	0	0	0	.4	.3	0	.2	.2	0	0	.1	0	0	.1	0
S_x				1.	.2	0	0	0	.1	0	0	0	0	0	0	0	0	.1
S_y					1.	.3	0	0	.3	0	0	.3	0	0	.1	0	0	.1
M_{yz}						1.	0	0	.1	0	0	0	0	0	.1	0	0	.1
δ_x							1.	.6	0	.4	.2	0	.6	.2	0	.3	0	0
δ_y								1.	0	0	.1	0	.1	.2	0	.3	.2	0
δ_z									1.	0	0	.4	0	0	.5	0	0	.8
$\dot\delta_x$										1.	.1	0	.9	.2	0	0	0	0
$\dot\delta_y$											1.	0	.2	.7	0	.1	.3	0
$\dot\delta_z$		SYMMETRIC										1.	0	0	.9	0	0	.1
$\dot\delta_{x/\ddot x}$													1.	.1	0	.2	.2	0
$\dot\delta_{y/\ddot x}$														1.	0	.1	.2	0
$\dot\delta_{z/\ddot x}$															1.	0	0	..3
$\dot\delta_{x/\ddot y}$																1.	.1	0
$\dot\delta_{y/\ddot y}$																	1.	0
$\dot\delta_{z/\ddot y}$																		1.

[redacted]

Figures 4-10 through 4-12 show the associated velocity errors representing error analyses for vehicles SA-9, SA-8, and SA-10, respectively.

([redacted] 4.3 CORRELATION BETWEEN GUIDANCE ERRORS

Table 4-I-V shows a typical set of correlation coefficients between the various guidance system errors. The values are given to the first decimal and were computed using the equation:

$$\rho_{ij} = \sigma_{ij}/\sigma_i\sigma_j$$

where: σ represents the elements of the covariance matrix associating velocity component errors to the guidance system errors.

i refers to the ith row and j refers to the jth column.

Although these values may vary between vehicles and also between computer runs due to weighting factors, three pairs of error terms are consistently highly ($\rho \geq 0.75$) correlated, (1) bias in X and scale factor in X, (2) constant drift of X gyro and "g" drift proportional to X, (3) constant drift of Z gyro and "g" drift proportional to X.

[redacted]) 5.0 CONCLUSIONS

The purpose of a postflight analysis of the guidance system is to establish the confidence in preflight error measurements and point out areas where improvements may be made. The predicted and postflight analysis platform system errors are shown in bar graph form in Figures 5-1 **and** 5-2. The asterisks over the particular errors indicate that predicted and analysis errors are opposite in sign.

Platform leveling and azimuth errors were predicted to be within 3σ tolerances of 0.005 and 0.01 degrees, respectively. The relative large values observed on SA-5, SA-6, and SA-7 are believed to be results of vibrations during thrust buildup. The platforms, which became space-fixed at liftoff signal, probably had moved due to vibrations and the gyro null positions were erroneously oriented at liftoff. Beginning with SA-9 the platforms were space-fixed prior to ignition and any torque applied to the platform during thrust buildup was sensed by the gyros and a torque equal and opposite in sign was generated thus stabilizing the platform. The leveling and azimuth errors shown for SA-9, SA-8 and SA-10 are well within the 3σ tolerances.

Figures 5-3 and 5-4 show the differences between computed and predicted platform system errors. In practically every case where the difference value is relatively large, the analysis indicated an error

[redacted]

opposite in sign to the prediction. The comparisons in general are very good and especially good if the sign convention is disregarded. The magnitudes of the errors determined from the postflight analyses were generally very close to predictions.

Considerations have been given to incorporating guidance error corrections in the flight equations to compensate for preflight measurments. Based on the results of the Saturn I Block II guidance error analyses, it is felt that effectively large accelerometer errors could be compensated for in the flight equations. However, gyro drift rate compensation would be questionable until some additional analyses are made using the flight data from vehicles carrying the ST-124 M platforms.

Table 5-I shows the averages of the guidance error comparisons (analysis minus prediction). These averages for the accelerometer error measurements, bias and scale factor, show that preflight estimates were generally good. The initial platform alignment errors for the last three vehicles were held within the 3α tolerances with an average value of $\pm 0.31 \times 10^{-2}$ degrees.

The average difference of the constant drift errors was slightly less than the 3σ value of 0.75 deg/hr. The average difference in the "g"-sensitive drifts was 0.07 deg/hr/g compared to a 3σ value of 0.05 deg/hr/g. However, if the sign convention is disregarded, the averages of the difference in magnitude would be 0.034 deg/hr and 0.038 deg/hr/g for constant and "g"-sensitive drifts, respectively.

The missions of the Saturn I Block II vehicles did not require more accurate guidance hardware. However, based on the comparisons shown previously, the use of advanced quality control techniques in selecting the individual components of the guidance system hardware already designed would insure the fulfilment of the terminal conditions to high degree of accuracy. Corrections for accelerometer errors could be programmed in the flight computer. Programming of corrections for gyro drifts would be somewhat questionable until tests show that "g"-sensitive drifts are more repeatable.

TABLE 5-I

(C) GUIDANCE ERROR COMPARISONS
(AVERAGE VALUES)

ERROR TERM	UNITS	SAMPLES	AVERAGE	(AVERAGE) *
Bias	m/s^2	18	$\pm 0.3 \times 10^{-3}$	
Scale Factor (all)	g/g	12	$\pm 0.28 \times 10^{-4}$	
Scale Factor (SA-9 excluded)	g/g	10		$(\pm 0.22 \times 10^{-4})$
Leveling and Azimuth (all)	degrees	18	$\pm 0.78 \times 10^{-2}$	
Leveling and Azimuth (SA-5,6 and 7)	degrees	9		$(\pm 1.15 \times 10^{-2})$
Leveling and Azimuth (SA-9,8 and 10)	degrees	9		$(\pm 0.31 \times 10^{-2})$
Constant Drift	deg/hr	18	± 0.072	
"g"-Drift	deg/hr/g	24	± 0.07	

*1. Due to approximately 4 degree lower than normal inertial gimbal temperature, postflight estimate of scale factor error was 0.768×10^{-4} g/g for vehicle SA-9.

2. Platform space-fixed at liftoff signal on vehicles SA-5, SA-6, SA-7. Platform space-fixed prior to ignition on vehicles SA-9, SA-8, SA-10.

[redacted]

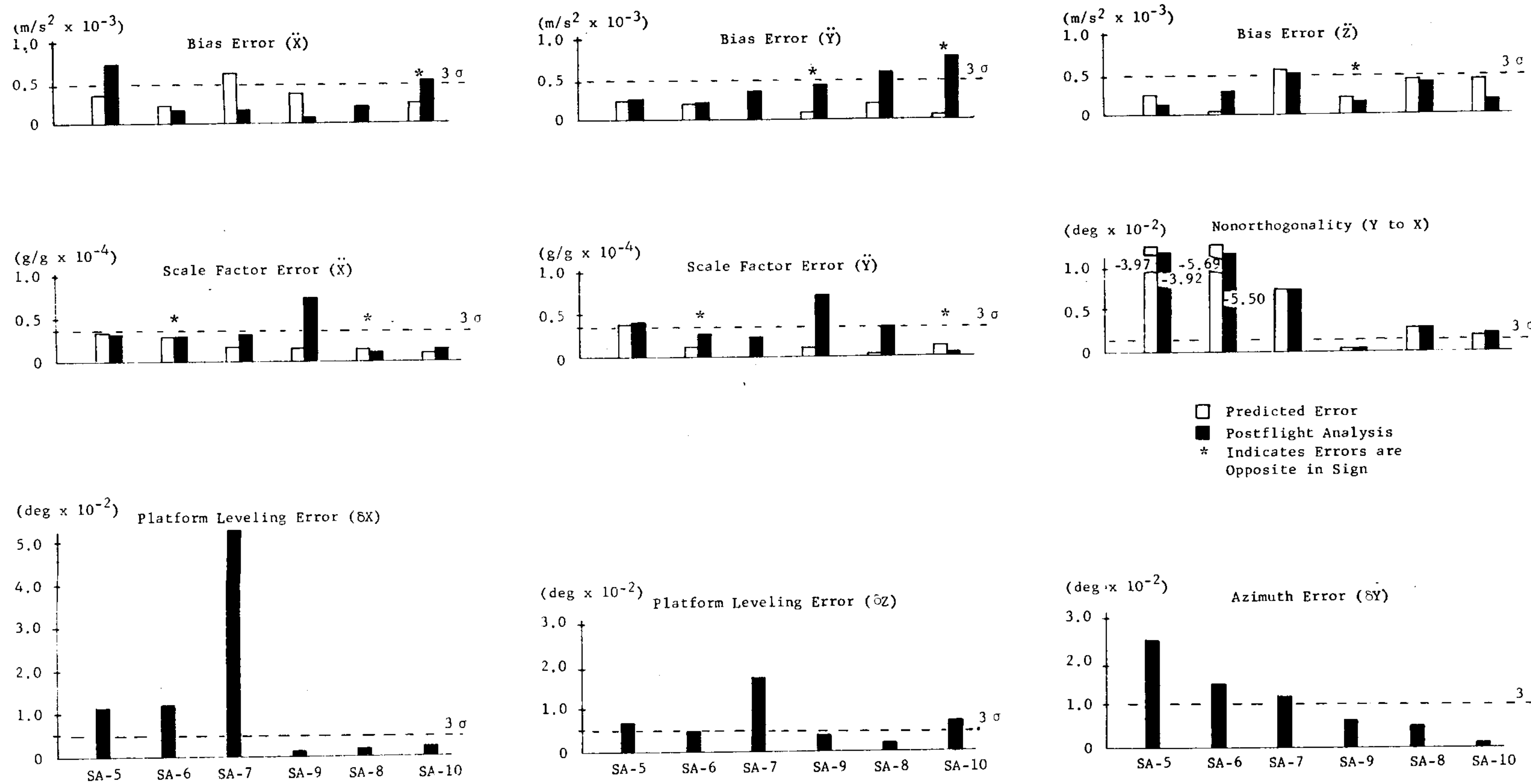

FIGURE 5-1 GUIDANCE ACCELEROMETER AND INITIAL ALIGNMENT ERRORS (PREDICTED AND POSTFLIGHT ANALYSIS)

[redacted]

[redacted]

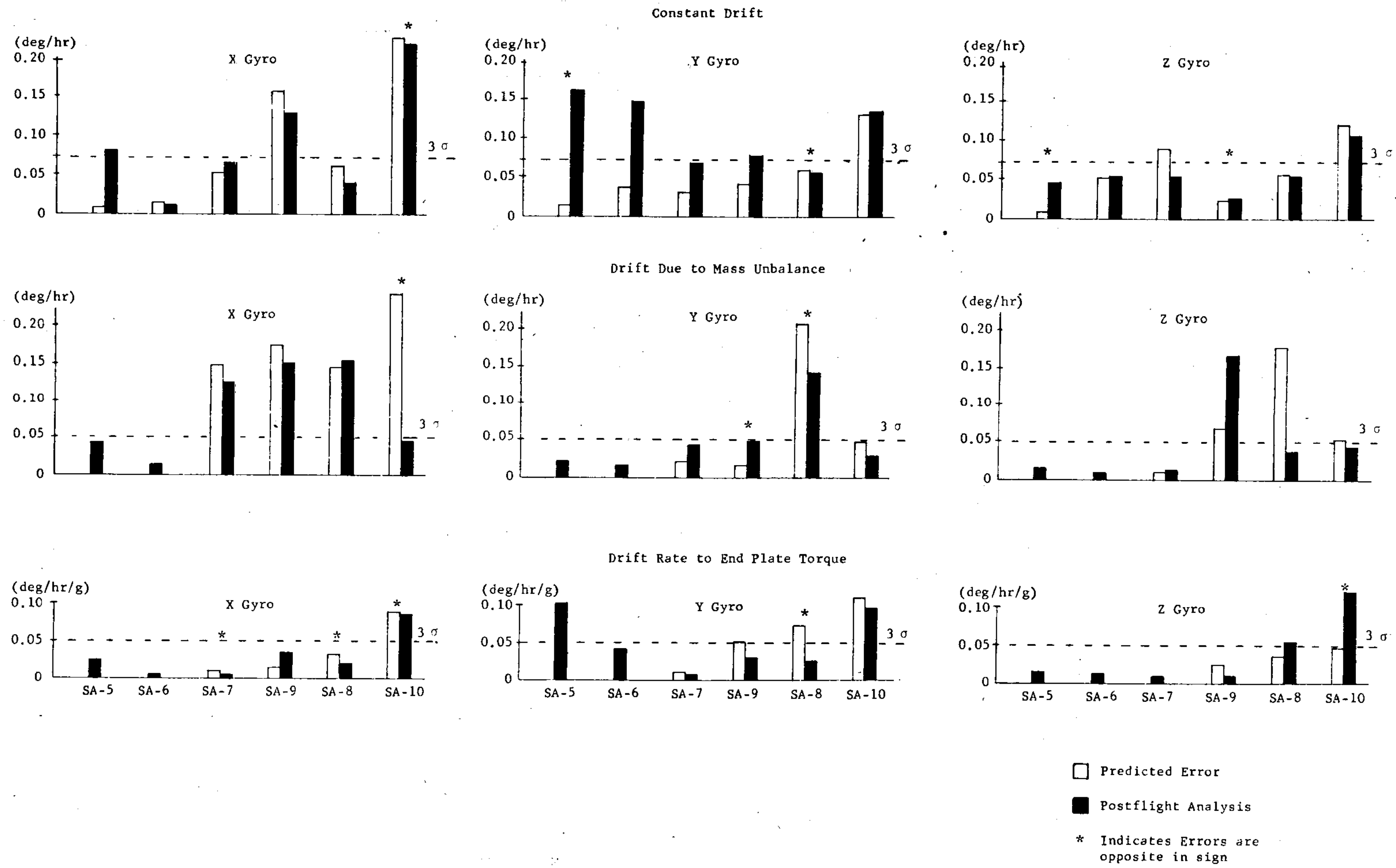

FIGURE 5-2 GYRO DRIFT RATES (PREDICTED AND POSTFLIGHT ANALYSIS)

[redacted]

[redacted]

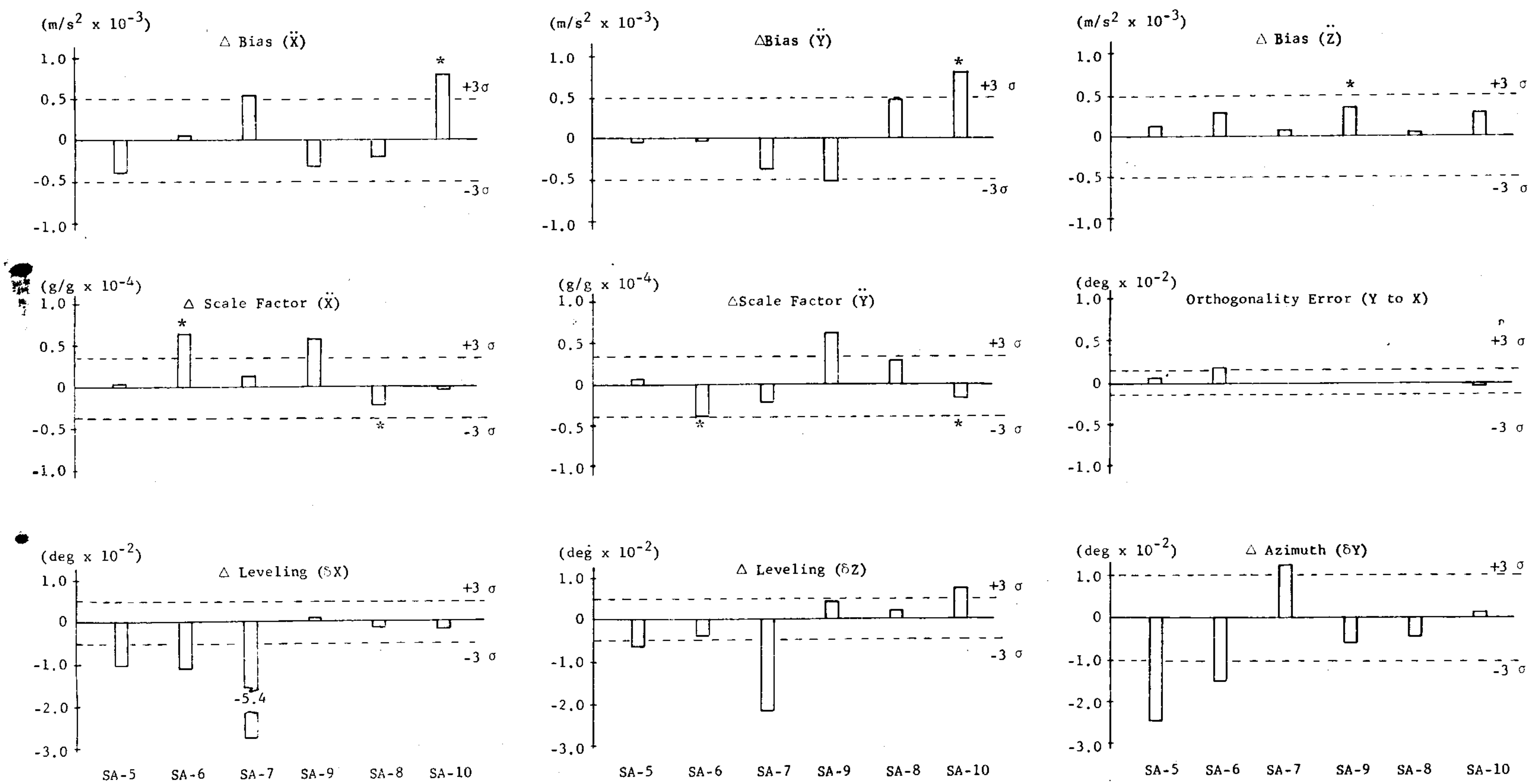

Note: * Indicates predicted and analysis errors have opposite signs

FIGURE 5-3 GUIDANCE ERROR COMPARISONS (ANALYSIS MINUS PREDICTED)

[redacted]

[redacted]

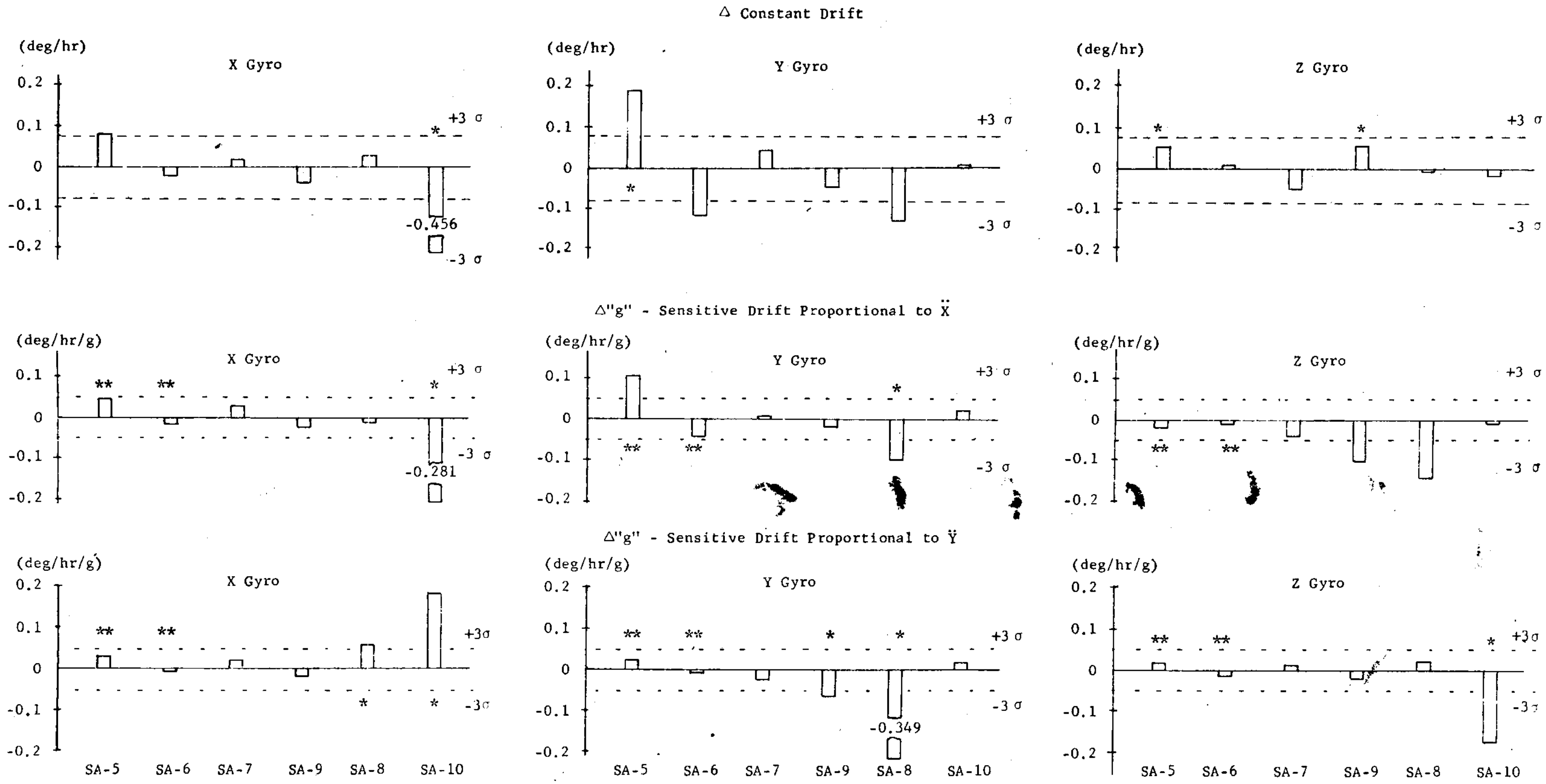

Note: * Indicates predicted and analysis error opposite sign

** Indicates predicted values were not available

FIGURE 5-4 GUIDANCE ERROR COMPARISONS (ANALYSIS MINUS PREDICTED)

[redacted]

[redacted]) REFERENCES

1. MPR-SAT-FE-64-15, April 1, 1964, Results of The Fifth Saturn I Launch Vehicle Test Flight ([redacted]), Saturn Flight Evaluation Working Group.

2. MPR-SAT-FE-64-16, August 7, 1964, Results of The Sixth Saturn I Launch Vehicle Test Flight ([redacted]), Saturn Flight Evaluation Working Group.

3. MPR-SAT-FE-64-17, November 25, 1964, Results of The Seventh Saturn I Launch Vehicle Test Flight ([redacted]), Saturn Flight Evaluation Working Group.

4. MPR-SAT-FE-65-6, April 30, 1965, Results of The Eighth Saturn I Launch Vehicle Test Flight ([redacted]), Saturn Flight Evaluation Working Group.

5. MPR-SAT-FE-65-6, July 27, 1965, Results of The Ninth Saturn I Launch Vehicle Test Flight ([redacted]), Saturn Flight Evaluation Working Group.

6. MPR-SAT-FE-65,14, September 24, 1965, Results of The Tenth Saturn I Launch Vehicle Test Flight ([redacted]), Saturn Flight Evaluation Working Group.

APPROVAL TM X-53398

SATURN I BLOCK II GUIDANCE SUMMARY REPORT

By R. A. Chapman

The information in this report has been reviewed for security classification. Review of any information concerning Department of Defense or Atomic Energy Commission programs has been made by the MSFC Security Classification Officer. The highest classification has been determined to be Confidential.

This report has been reviewed and approved for technical accuracy.

Carlos C. Hagood
Chief, Flight Evaluation Branch

James P. Lindberg
Chief, Flight Evaluation and
Operations Studies Division

Dr. E. D. Geissler
Director, Aero-Astrodynamics
Laboratory

DISTRIBUTION

Dr. Rees, DEP-T

I
Col. James, I-I/IB-MGR
Dr. Speer, I-MO-MGR

R&D
Mr. Weidner, R-DIR

R-AERO
Dr. Geissler, R-AERO-DIR
Mr. Jean, R-AERO-DIR
Mr. Lindberg, R-AERO-F
Mr. Hagood, R-AERO-FF
Mr. Stone, R-AERO-FM
Mr. McNair, R-AERO-P
Mr. Winch, R-AERO-DA
Mrs. Chandler, R-AERO-DAG
Mr. Sheats, R-AERO-FFR
Mr. Chapman, R-AERO-FFR (10)
Mr. Horn, R-AERO-D
Mr. Hart, R-AERO- G
Mr. Baker, R-AERO-G

R-ASTR
Dr. Haeusserman, R-ASTR-DIR
Mr. Ferrell, R-ASTR-GSA
Mr. Nicaise, R-ASTR-NGI
Mr. Mandel, R-ASTR-G
Mr. Mack, R-ASTR-S
Mr. Digesu, R-ASTR-A
Mr. H. Thomason, R-ASTR-G
Mr. Moore, R-ASTR-N
Mr. S. Seltzer, R-ASTR-NG

R-COMP
Mr. Houston, R-COMP-RRM (2)

MSC
Mr. Henson, MSC-EG

EXTERNAL
International Business Machines
System Design, Dept. 229
150 Sparkman Drive NW
Huntsville, Alabama 35808
Attn: R. E. Poupard (2)
Ron Avery (1)

CC-P
I-RM-M
MS-H
MS-IP
MS-IL (8)
MS-T
Mr. Bland (5)
Mr. Bulette

Scientific and Technical Information Facility (25)
Attn: NASA Representative (S-AK/ RKT)
P. O. Box 33
College Park, Maryland 20740

C. A. Cassoly
Projects Aeronautical Material Laboratory
Naval Aeronautical Engineering Center
Philadelphia 12, Pa.